The Effect of Pressure on the Mechanical Properties of Polymers

R. W. Fillers and N. W. Tschoegl

Citation: Transactions of The Society of Rheology (1957-1977) **21**, 51 (1977); doi: 10.1122/1.549463
View online: http://dx.doi.org/10.1122/1.549463
View Table of Contents: http://scitation.aip.org/content/sor/journal/tsor/21/1?ver=pdfcov
Published by the The Society of Rheology

TRANSACTIONS OF THE SOCIETY OF RHEOLOGY 21:1, 51–100 (1977)

The Effect of Pressure on the Mechanical Properties of Polymers

R. W. FILLERS* and N. W. TSCHOEGL, *Division of Chemistry and Chemical Engineering, California Institute of Technology, Pasadena, California 91125*

Synopsis

Stress relaxation measurements were made as a function of temperature and hydrostatic pressure on two lightly filled elastomers (Hypalon 40 and Viton B), one highly filled elastomer (Neoprene WB), and on an EPDM rubber. The latter was not piezorheologically simple. The lightly filled elastomers showed piezorheologically simple behavior, i.e. their response curves under different hydrostatic pressures could be superposed empirically by a simple horizontal shift along the logarithmic axis. The filled elastomer was piezorheologically simple only in the rubbery region and in the beginning of the transition region. The dependence of the empirical shift distances, log a_p, on P could not be described by either the Ferry–Stratton or the Bueche–O'Reilly equation. By considering the bulk modulus to be linearly related to pressure, a new equation has been developed for log $a_{T,P}$ which describes the pressure dependence well and contains the WLF equation as a limiting case. Published data on the response of poly(vinyl chloride) under superposed hydrostatic pressure are shown to obey the new equation also.

The theoretical importance of the new equation lies in the fact that combination of the usual isobaric measurements at atmospheric pressure as function of temperature with isothermal measurements as function of pressure allows, in principle, all the molecular parameters required by the free volume theory to be determined unambiguously.

INTRODUCTION

While the effect of temperature on the mechanical properties of amorphous solid polymers is fairly well understood, relatively little information is available on the effect of pressure. It is well estab-

*Present address: Aerospace Corporation, P.O. Box 92957, Los Angeles, Calif. 90009.

lished that the viscosity of simple liquids increases with the application of a hydrostatic pressure.[1,2] Tensile measurements on elastomers by Patterson[3] under superposed hydrostatic pressure clearly showed that the effect of increasing pressure on Young's modulus was similar to the effect of decreasing temperature, i.e., glass-like behavior is encountered above a transition pressure P_g (more accurately a transition interval characterized by P_g). The existence of a pressure transition in polymers has been discussed by various authors[4–6] and now appears to be universally accepted.

The pressure dependence of the mechanical response has been predicted theoretically on the basis of the free volume approach by Ferry and Stratton[7] who derived the pressure analog of the well-known WLF equation[8,5] in the form

$$\log a_P = \frac{(B/2.303f_0)\ (P - P_0)}{f_0/\kappa_f - (P - P_0)}, \tag{1}$$

where a_P is the ratio of the relaxation times at pressure P to the relaxation times at a reference pressure P_0; B is a constant assumed to be of the order of unity; f_0 is the fractional free volume at the reference pressure; and κ_f is the isothermal compressibility of the free volume. Other investigators[9,10] have proposed the equation

$$\log a_P = C(P - P_0), \tag{2}$$

where C is a constant. Neither equation has so far been subject to extensive mechanical testing on solid polymers.

Zosel[11] made shear stress relaxation measurements in a torsion pendulum to study the effect of superposed hydrostatic pressures up to 1,000 atmospheres on the mechanical properties of poly(vinyl chloride). His results could not be described satisfactorily by either eq. (1) or eq. (2).

Other investigations have also utilized the torsion pendulum to study the effect of pressure on the isochronal shear modulus and loss tangent of a variety of polymers, including elastomers.[12,13] Stress relaxation and creep measurements on polyethylene have also been carried out[14] at pressures up to 2 kbar. Again, these measurements have not been extensive enough to allow testing of eqs. (1) and (2). O'Reilly found[10] that eq. (2) described the pressure dependence of his dielectric relaxation data on poly(vinyl acetate). However,

Sasabe[15] concluded from dielectric measurements on several polymers that eq. (2) fails at higher pressures.

The complex bulk modulus (or the complex bulk compliance) of several polymers, including some elastomers, has been the subject of important investigations by McKinney, Belcher, and Marvin.[16,17] In the work reported here we are concerned with the effect of pressure on the (time-dependent) shear or tensile modulus. Thus the work of Marvin and collaborators, as well as the many investigations concerned with the establishment of PVT relations,[18–27] is not of direct interest to us here. The same applies to studies of the ultimate behavior of polymers which have recently been reviewed by Radcliffe.[28] In general, these investigations have not been concerned with the time-dependent properties, but specifically with the influence of pressure on the elastic response and the yield and fracture criteria.

This paper reports on stress relaxation measurements in simple tension performed under superposed hydrostatic pressures up to 5 kbar and temperatures generally ranging between $-25°$ and 44°C on four elastomers: Hypalon 40®, Viton B®, Neoprene WB®, and EPDM. These materials were chosen because their pressure transitions lay within the useful pressure range of the apparatus. The measurements led to the development of a time-temperature-pressure superposition principle expressible in the form of a new equation which includes the WLF equation as a limiting case. It is also shown that combination of the usual isobaric measurements at atmospheric pressure as function of temperature with isothermal measurements as function of pressure allows the unambiguous determination of B and f_0, and of the expansivity and the compressibility parameters of the free volume.

EXPERIMENTAL

Materials

Hypalon 40, Viton B, and Neoprene WB were graciously supplied by E. I. du Pont de Nemours and Co., Inc. Their compounding recipes are reported in Appendix I; a more complete discussion of these materials is given by Stevenson.[29] Briefly, Hypalon 40, a

® Trademark of E. I. du Pont de Nemours Co., Inc.

chlorosulfonated polyethylene, is lightly filled with 4 phr SRF carbon black. Viton B, a copolymer of vinylidene fluoride and hexafluoropropylene, is also lightly filled with 20 phr MT carbon black. The Neoprene WB is a polychloroprene rubber which contains 100 phr MT carbon black and 25 phr hard clay, and it was included to obtain the response of a highly filled system. The EPDM elastomer was prepared by curing 100 parts U.S. Rubber Co. Royalene 301T® with a 3 phr Di-cup R®. Royalene 301T is an ethylene–propylene copolymer containing a controlled amount of non-conjugated diene. Di-cup R is a 98–99% active dicumyl peroxide manufactured by Hercules, Inc.

Specimens were cut with a knife edge mill blade. Their dimensions were 14.0 cm (5.5 inch) long, 0.20 cm (0.080 inch) thick, and ranged from 0.20 to 0.95 cm (0.080 to 0.375 inch) in width. U-shaped copper clips were cemented over approximately 0.64 cm (0.25 inch) at each end.

Apparatus

On the basis of the work of Patterson[3] the apparatus was designed to measure stress relaxation up to 8 kbar to enable measurements to be made on natural rubber and on styrene–butadiene rubber. Unfortunately, the trigger mechanism would not operate reliably above approximately 5 kbar. To avoid a time consuming major redesign of the relaxometer, the work was switched to the four elastomers listed in the preceding section.

The experimental arrangement is shown in Figure 1 below. P_1 indicates a thermostat containing the pressure vessel which houses the stress relaxometer. The pressure is applied using a low pressure hand pump (H_1) for the initial compression and a high pressure hand pump (H_2) for the final compression. A Bourdon tube gage (G) monitors the pressure on the low pressure side of the system. A reservoir (R_2) contains a supply of hydraulic fluid for the pumps. A 10:1 intensifier (I) yields a pressure boost of approximately 9:1 after accounting for frictional losses. The high pressure side of the system must be primed to about 350 bar before using the intensifier. The 1:1 separator (S) allows the system to be primed without contamination of the silicone oil used as pressurizing fluid in the high pressure side of the system with the hydraulic fluid used in the low pressure side. Another reservoir (R_1) contains a supply of the sili-

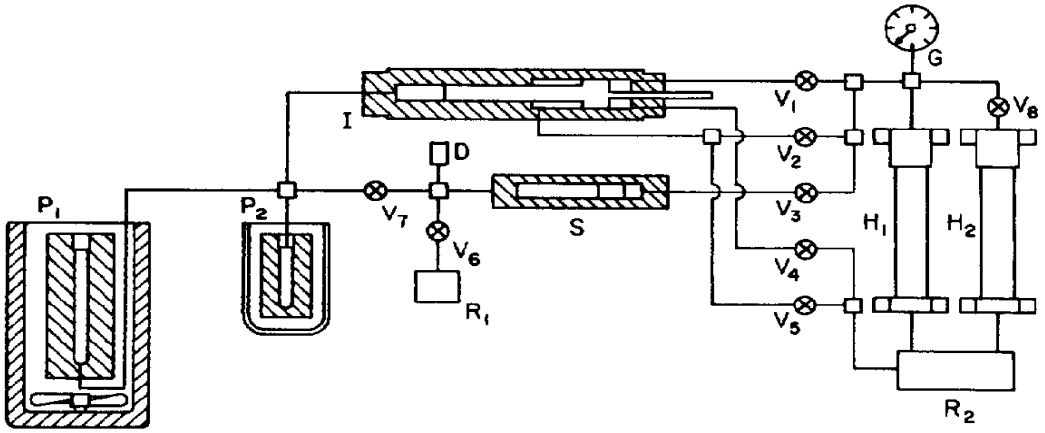

Fig. 1. Experimental arrangement.

cone oil. The pressure on the high pressure side is measured by a high pressure gage (see below) placed into a second high pressure vessel (P_2). A rupture disk (D) functions as a safety valve.

The pressure vessel is submerged in a continuously stirred silicone fluid bath whose temperature is controlled within $\pm.02$°C by a proportional controller. A platinum resistance thermometer placed inside the pressure vessel serves to calibrate the thermal lag across its walls; once determined, the temperature is measured with either a mercury thermometer or with a differential thermocouple placed in the bath. The high pressure gage consists of a 64 ohm manganin coil prepared and seasoned according to Babbs and Scott.[30] This coil is maintained at 0°C. Its resistance is measured with a Mueller bridge and a galvanometer. The high pressure measuring system was calibrated with a Heiss Bourdon tube gage. This arrangement is estimated to yield an absolute error of 0.1%, with a relative error of 0.05% between 1 bar and 5 kbar pressure, since the manganin coil is much more sensitive than the Bourdon tube gage.

The stress relaxometer and the pressure vessel in which it is installed are shown in Figure 2. The stress relaxometer (Fig. 2a) consists of two spring-loaded concentric cylinders (I and 0) between which the specimen (E) is held. A removable snap-ring (SR) allows springs of various stiffness to be inserted between the cylinders, depending upon the force required. A small hole (H) drilled through the copper strips cemented to the ends of the specimen allows its attachment to the removable end cap (C). The specimen is then lowered into the

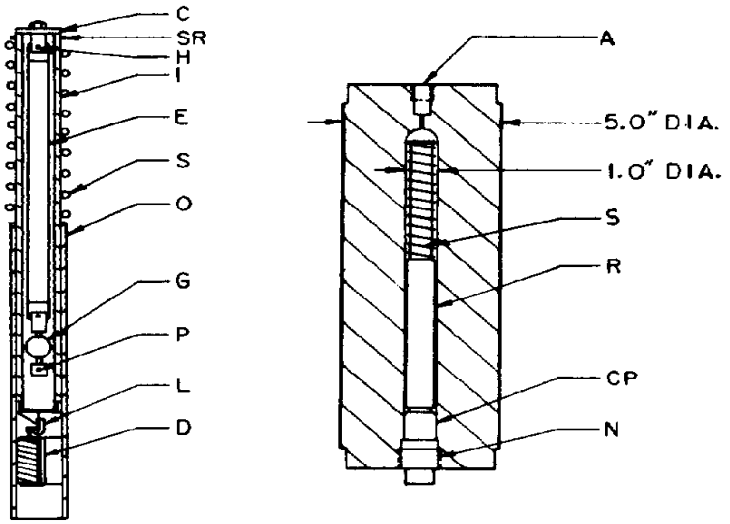

Fig. 2. Stress relaxometer (a) and pressure vessel (b).

cylinders and attached to the bottom clevis (G) with a screw-pin. The bottom clevis assembly is attached to the outer cylinder via a dowel pin (P). The inner cylinder is slotted for this pin, allowing vertical travel without rotation. Pre-stressing the spring (S) forces the two cylinders apart until the bottom cap engages the dowel pin. Spacers of various thickness are inserted in this space to change the amount of travel, and consequently, the displacement of the specimen. When the two cylinders are pressed together, a hook machined on the bottom cap engages the latch (L). The latch is shaped in such a manner that the mechanism is triggered when the solenoid (D) is activated. In practice, the proper combination of spring and spacer is chosen so that the energy of the compressed spring is greater than the energy required to extend the specimen. When this condition is satisfied, the cylinders are extended until the bottom cap of the inner cylinder engages the dowel pin. The specimen is extended simultaneously and held fixed throughout the experiment. The (relaxing) force generated in the specimen by the extension is then measured via two strain gages incorporated in the lower clevis assembly (G). The gages were calibrated at various pressures and temperatures by replacing the specimen with a coil spring of known spring constant.

The pressure vessel (Fig. 2b) consists of a 40.64 cm (16 inch) long beryllium copper cylinder of 12.7 cm (5 inch) outer and 2.54 cm (1 inch) inner diameter. The relaxometer (R) is held in position by the closure plug (CP) which, in turn, is secured by the stainless steel nut (N). Both vessels use special cone connections (A) for connecting the vessels to the high pressure line.

The bottom closure plug (CP) contains the electrical leads for the strain gages and the solenoid. The pressure seal is fashioned according to Warschauer and Paul.[31] A standard O-ring forms the initial seal. Expansion of a beveled ring with increasing pressure forms a seal at the higher pressures. The plug, ring, and cones are made of beryllium copper. The seals endured about 40 pressurization cycles after which they had to be routinely rebuilt.

More details of the construction of the apparatus are given elsewhere.[32]

Experimental Procedure and Data Reduction

All experiments were performed after the establishment of equilibrium at each temperature and pressure. The approach to equilibrium was monitored by the strain gage output since lowering the temperature or increasing the pressure always slightly preloaded the specimen because of volume contraction. Most experiments were performed twice at each temperature and pressure, using different extensions to check the linearity of the response.

The experimentally measured quantities were the initial length, L_0, of the specimen, its stretched length, L, and the output voltage of the strain gage measuring the time-dependent force, $f(t)$. The strain, ϵ_0, was obtained from

$$\epsilon_0 = (L - L_0)/L_0. \tag{3}$$

The stress, $\sigma(t)$, was determined by dividing the force by the cross-sectional area of the specimen. Equation (19), which is discussed in the results section, was used to correct the initial cross-sectional area of the specimen to the area existing at the experimental temperature and pressure. Since the extension of the specimen requires a finite time, t_1, initial portions of the response, covering a time interval of about $10t_1$ to $25t_1$, were discarded.

The time-dependent tensile moduli at the temperature and pressure of the experiment, $E(t)$, were obtained from

$$E(t) = \sigma(t)/\epsilon_0 \tag{4}$$

and were reduced to the shear moduli at the same temperature and pressure, $G(t)$, for the reasons and in the manner explained in the next section. The shear moduli at temperature T and pressure P were then referred to the values they would have at the reference temperature T_0 and the reference pressure P_0. According to the theory of reduced variables,[5,33] the modulus in the reference state, $_R(t)$, is obtained from $G(t)$ by

$$G_R(t) = G(t)T_0\rho_0^0/T\rho, \tag{5}$$

where ρ is the density at temperature T and P, and ρ_0^0 is the density at the reference pressure and temperature. We have applied this correction although it is questionable whether it should be used at temperatures at which the material shows transition or glassy behavior. Because of the relatively small temperature range (at most 70°C) the temperature correction is slight in any case.

We took the effect of pressure into account by considering that $\rho_0^0/\rho = V/V_0^0$ where V is the volume at temperature T and pressure P and V_0^0 is the volume in the reference state, and applying the Murnaghan equation (19) to obtain the volume at pressure P. Sharda and Tschoegl[34] have recently shown that ρ_0^0/ρ should be replaced by $(V/V_0^0)^{-\gamma}$, where γ is a material parameter whose value is 0.2 for natural rubber. We do not know the value of γ for our materials. In any case, the difference between V/V_0^0 and $(V/V_0^0)^{-\gamma}$ is quite small because V/V_0^0 is close to unity.

Reduction to Shear Relaxation Modulus

The tensile mode was chosen for its experimental simplicity. For the establishment of a time-temperature-pressure superposition principle this mode, unfortunately, has theoretical drawbacks. For isothermal–isobaric segments of $E(t)$ to superpose by horizontal shifts along the logarithmic time axis it is necessary that changes in temperature and pressure affect all relaxation times in the same manner. This, however, is a necessary, but not a sufficient condition. In addition, the effect of temperature and pressure on the modulus at

any fixed time must be known to allow correction of the isothermal–isobaric segments before shifting.

It is shown in elasticity theory that the tensile modulus, E, is given in terms of the shear and bulk moduli, G and K, by

$$E = \frac{9KG}{3K + G}. \tag{6}$$

Thus the tensile modulus is a combination of the two fundamental moduli, G and K, which refer to changes in shape and size, respectively. In the rubbery region it is reasonable to assume that $G \ll K$, i.e. that the rubber is incompressible. In this case $E = 3G$ and the temperature and pressure dependence of E will be the same as that of G regardless of the temperature and pressure dependence of K. In the rubbery region, therefore, $E(t)$ and $3G(t)$ can be used interchangeably. This simplification is not available in the transition and glassy regions. In particular, while the shear relaxation modulus, $G(t)$, may be considered to be independent of the pressure, at least in a first approximation, this is clearly not true of $K(t)$, the bulk relaxation modulus. It appears preferable, therefore, to base any investigation of the time-temperature-pressure superposition of the mechanical properties of a polymer on shear relaxation data. For this reason our $E(t)$ data at any given temperature, T, and pressure, P, were converted to $G(t)$ data at the same temperature and pressure by the use of the equation

$$G(t) \simeq \frac{E(t)}{3[1 - E(t)/9K(T, P)]}, \tag{7}$$

which is discussed in Appendix II. Equation (7) is not exact. The cause of this will be discussed later. In eq. (7)

$$K(T, P) = K^*(T) + kP, \tag{8a}$$

where k is a material constant presumed to be independent of temperature and $K^*(T)$ is the bulk modulus at temperature T and zero pressure. Equation (8a) expresses the well-established experimental observation[35] that the equilibrium bulk modulus is a linear function of the pressure. The temperature dependence of the zero-pressure equilibrium modulus may be given with excellent approximation[36,25] by

$$K^*(T) = K^*_0 \exp [-m\alpha^*(T - T_0)], \tag{8b}$$

where m is another material constant, α^* is the thermal expansivity at zero pressure, and K^*_0 is the equilibrium bulk modulus at zero pressure and at the reference temperature T_0. The values of the various material constants employed in the conversion from $E(t)$ to $G(t)$ by eq. (7) are tabulated for the four test materials in Table I.

Effect of Pressurizing Medium

Dow Corning 200 silicone oil of 5 centistoke viscosity served as the pressurizing fluid. It is possible that the silicone oil would swell the specimen (particularly at higher pressures) and that this might affect the relaxation behavior. We do not know of any way to test this possibility directly. We obtained reassuring evidence to the contrary by comparing the weights of natural rubber specimens that were merely immersed in the silicone oil with those of others that were subjected to pressures of 7 kbar for several days. The latter were weighed immediately after they were recovered from the pressure vessel, before any appreciable diffusion could have taken place. Analysis of the data showed no statistically significant difference in weights.

Relaxation measurements were also made in an Instron tester on specimens treated in a similar way. The measurements were made at $-55°$ and $-60°$C, i.e. in the transition region close to the glass transition temperature of natural rubber where the response is steepest. There was essentially no difference between the curves determined on unpressurized and on pressurized specimens. The largest shift observed corresponded to that caused by a temperature difference of about 1°C.

RESULTS

The reduced isothermal-isobaric moduli, $G_R(t)$, are plotted as functions of time, t, in logarithmic coordinates in Figures 3 to 6 for Hypalon 40 and in Figures 7 to 10 for Viton B. Figures 3 and 7 show data segments obtained under different pressures at 25°C. Figures 4 and 8, 5 and 9, and 6 and 10, respectively, show data segments obtained at different temperatures at the pressures of 1, 1000, and 2000 bar, respectively.

Mastercurves were constructed by shifting the isothermal–isobaric data segments into superposition along the log t axis. Curves (A),

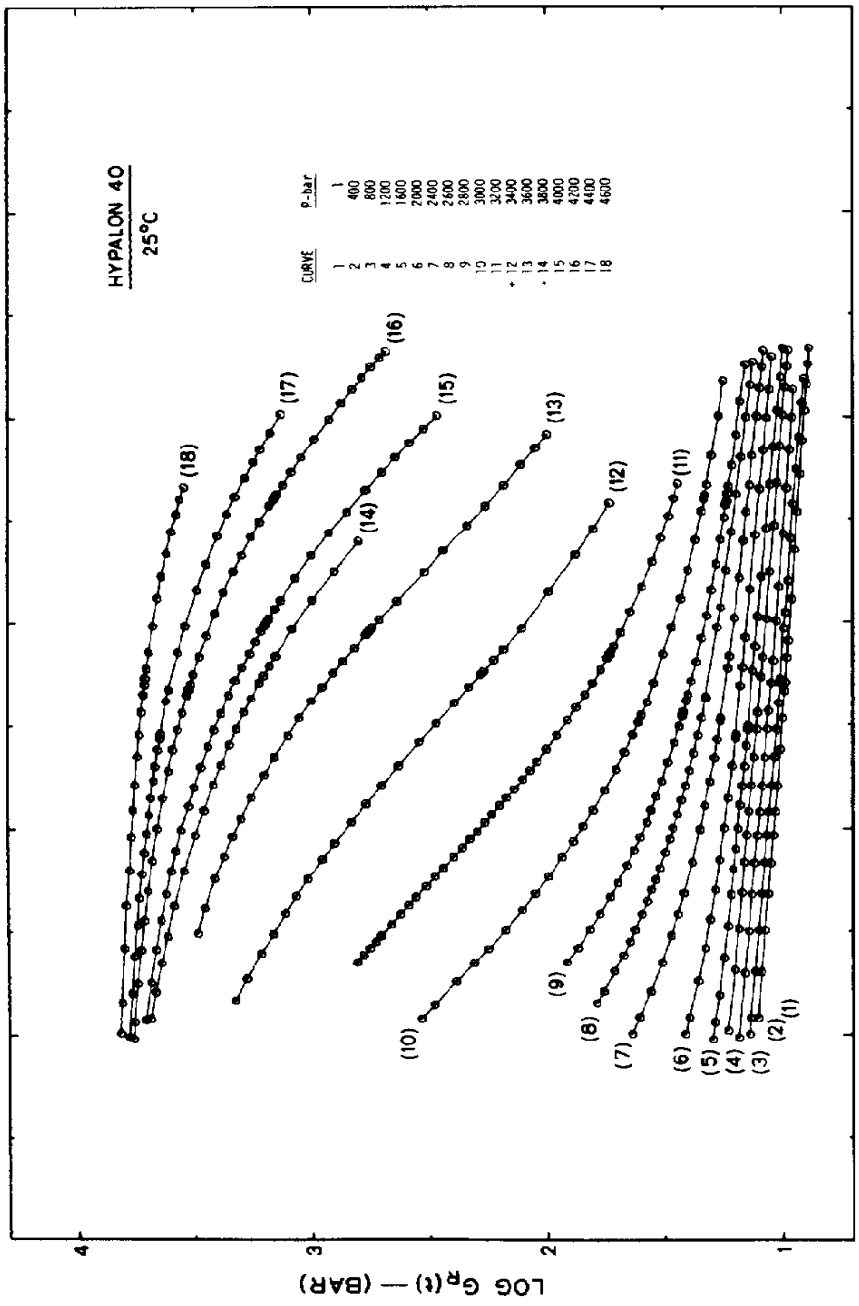

Fig. 3. Hypalon 40: shear modulus, $G_R(t)$, at $T = 25.0°C$ and pressures as indicated.

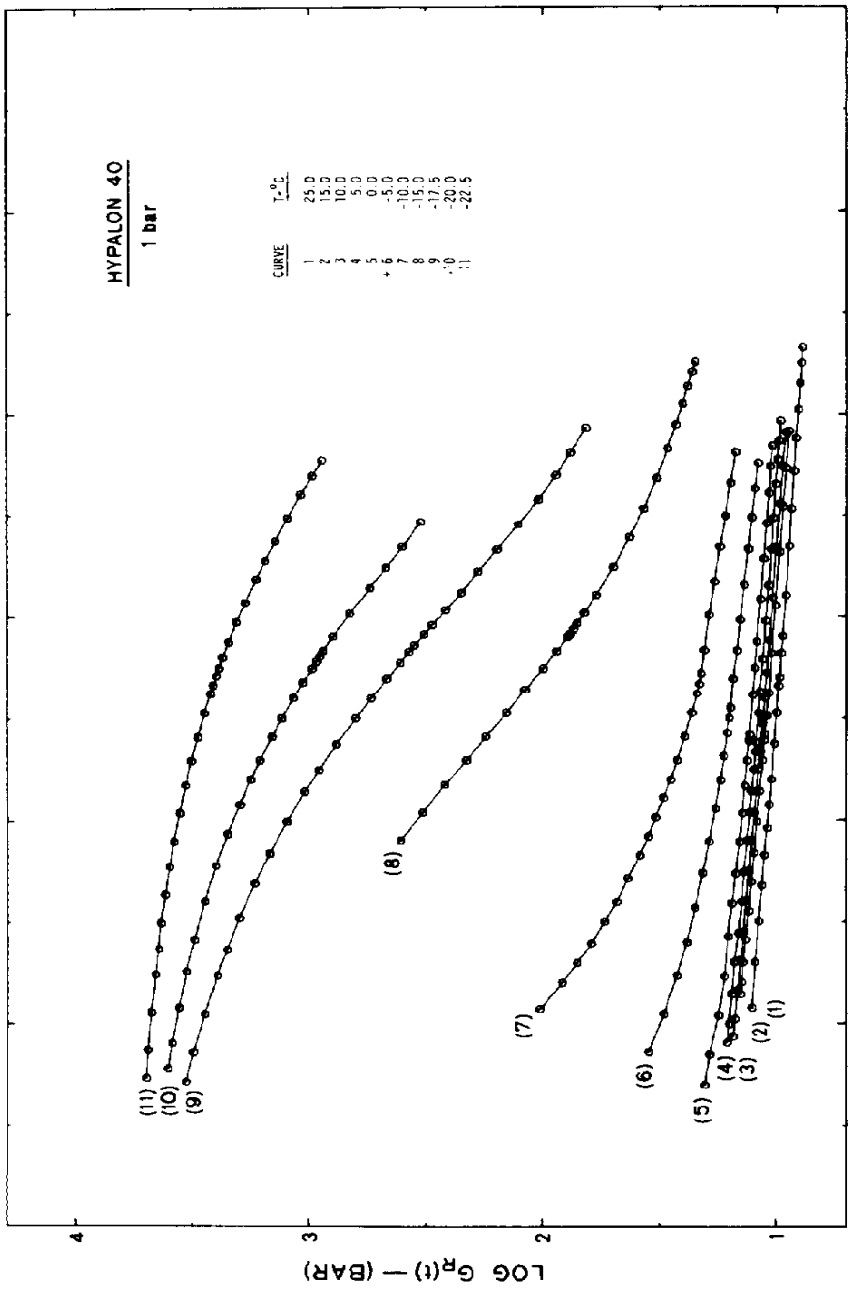

Fig. 4. Hypalon 40: shear modulus, $G_R(t)$, at $P = 1.0$ bar and temperatures as indicated.

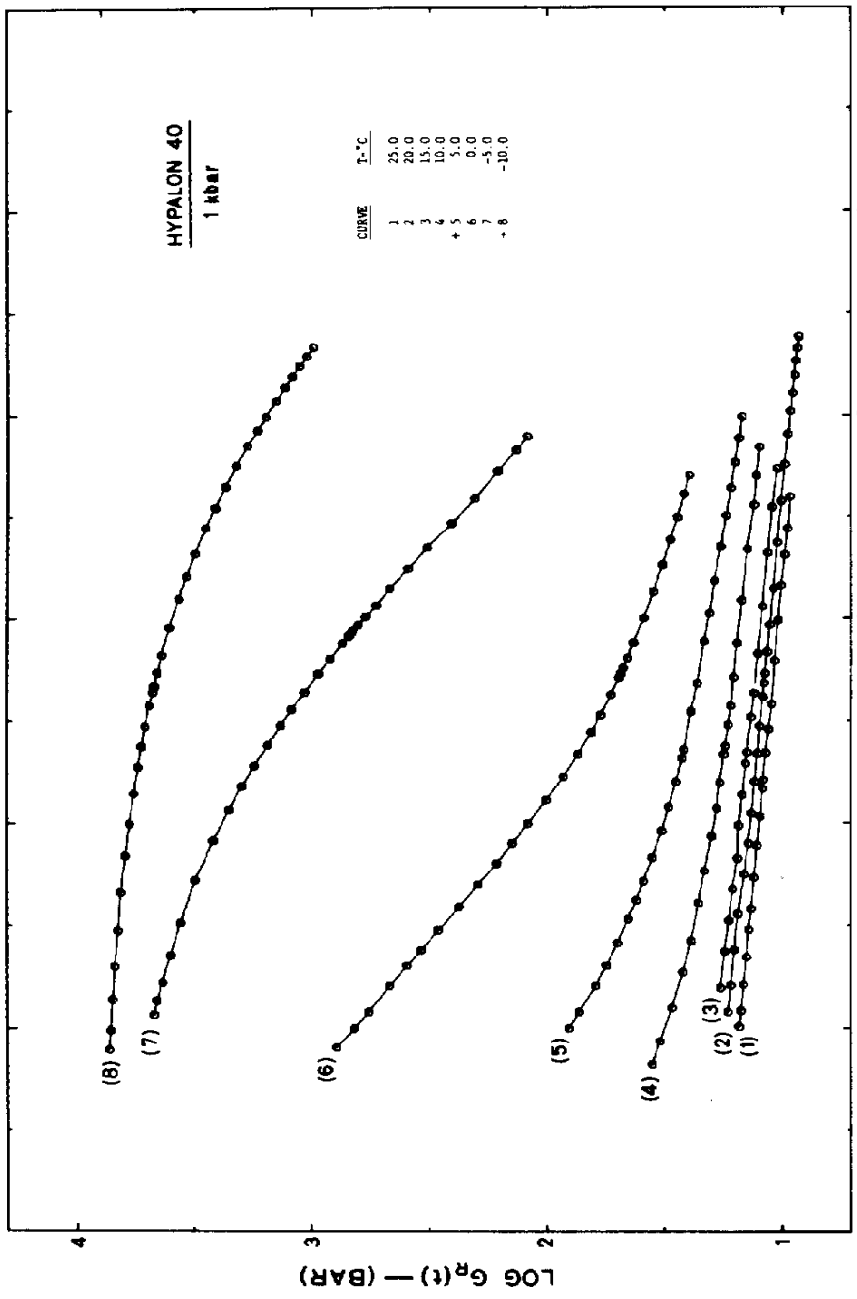

Fig. 5. Hypalon 40: shear modulus, $G_R(t)$, at $P = 1{,}000$ bar and temperatures as indicated.

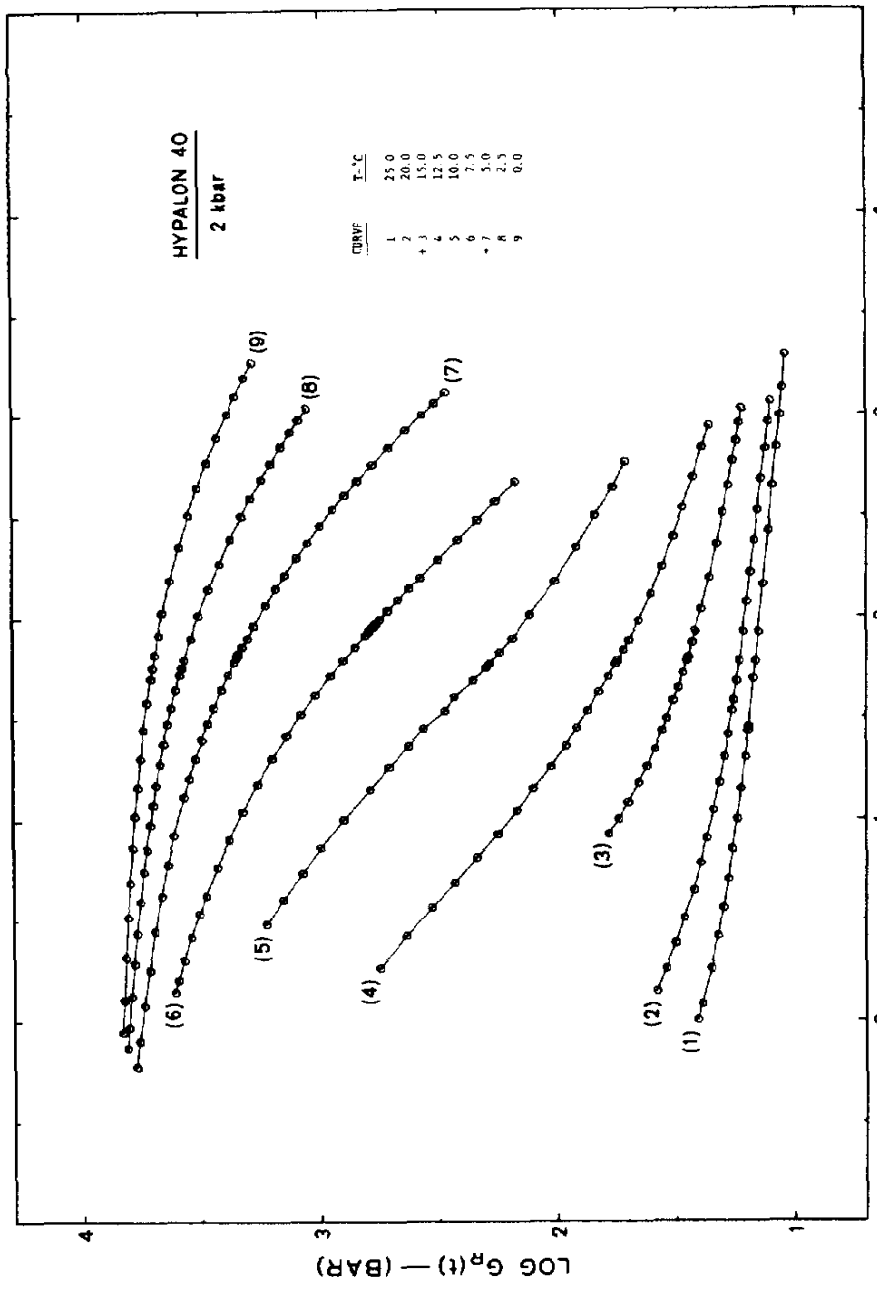

Fig. 6. Hypalon 40: shear modulus, $G_R(t)$, at P = 2,000 bar and temperatures as indicated.

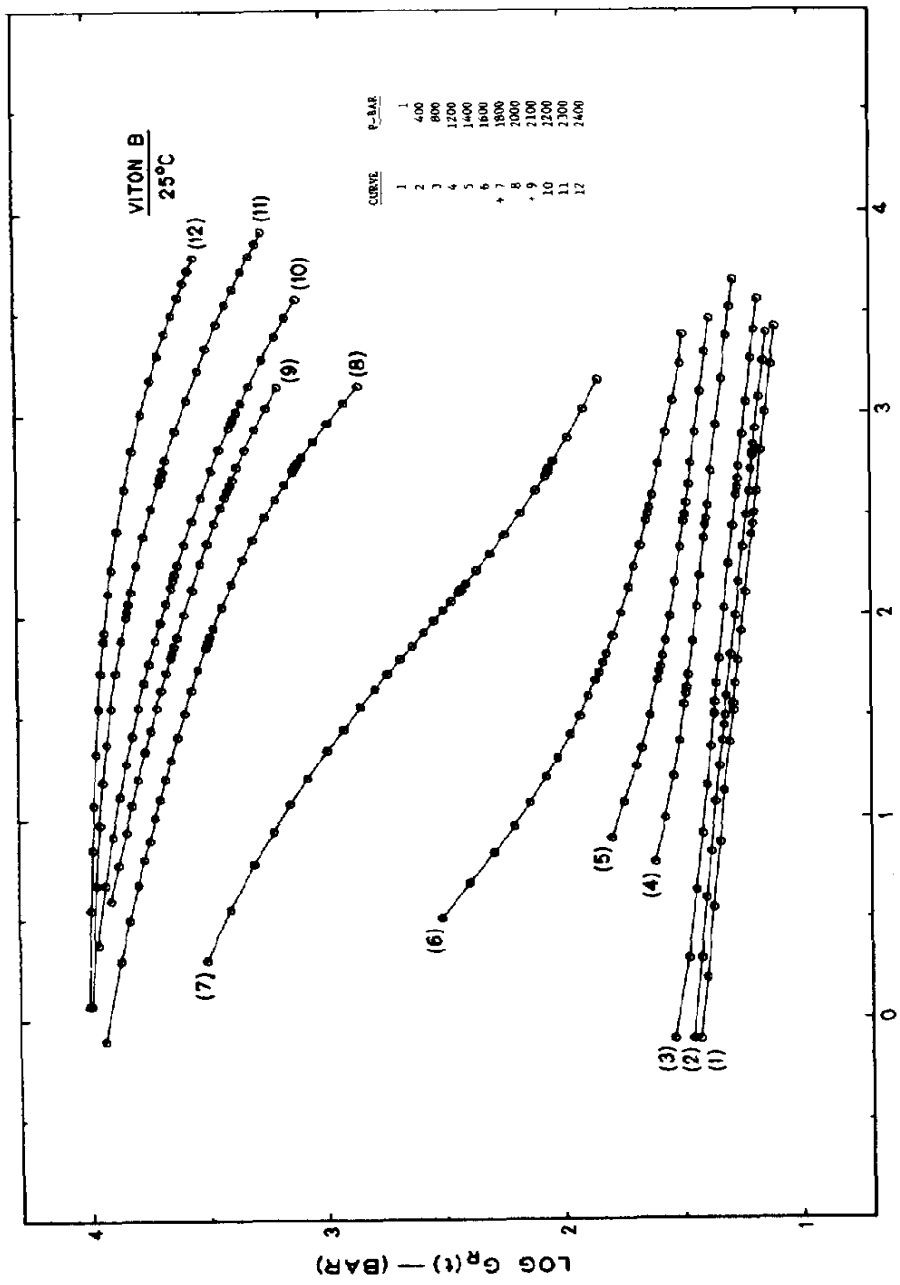

Fig. 7. Viton B: shear modulus, $G_R(t)$, at $T = 25.0°C$ and pressures as indicated.

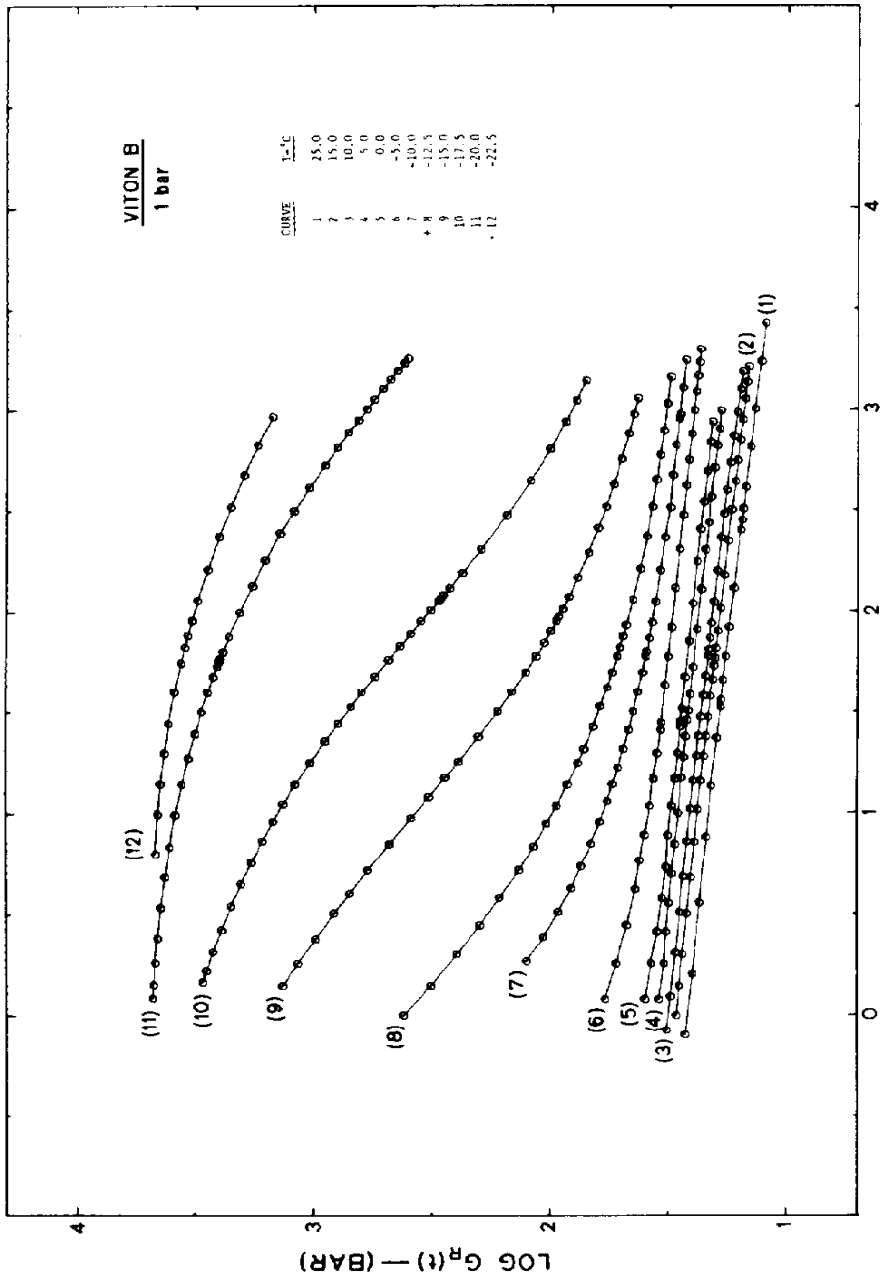

Fig. 8. Viton B: shear modulus, $G_R(t)$, at $P = 1.0$ bar and temperatures as indicated.

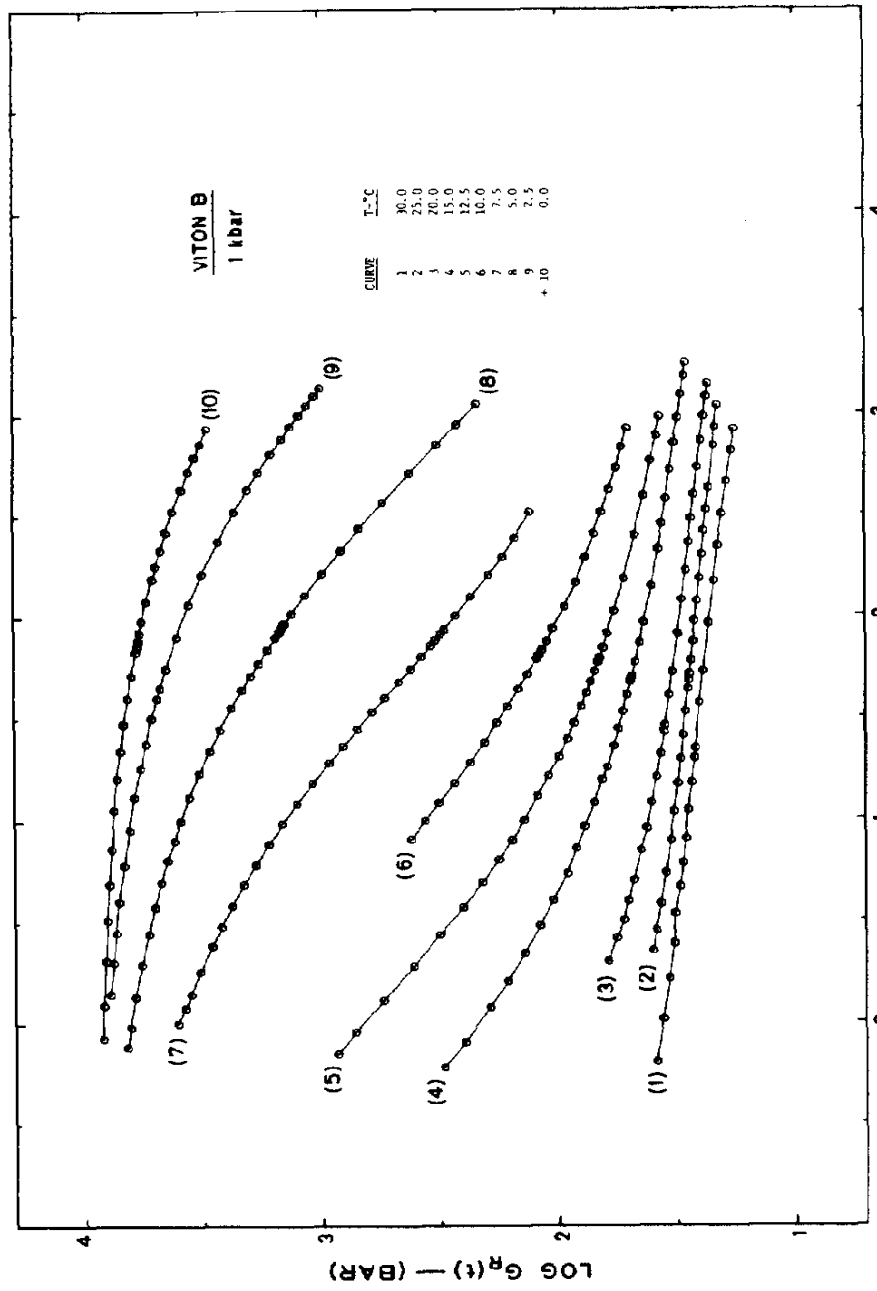

Fig. 9. Viton B: shear modulus, $G_R(t)$, at P = 1,000 bar and temperatures as indicated.

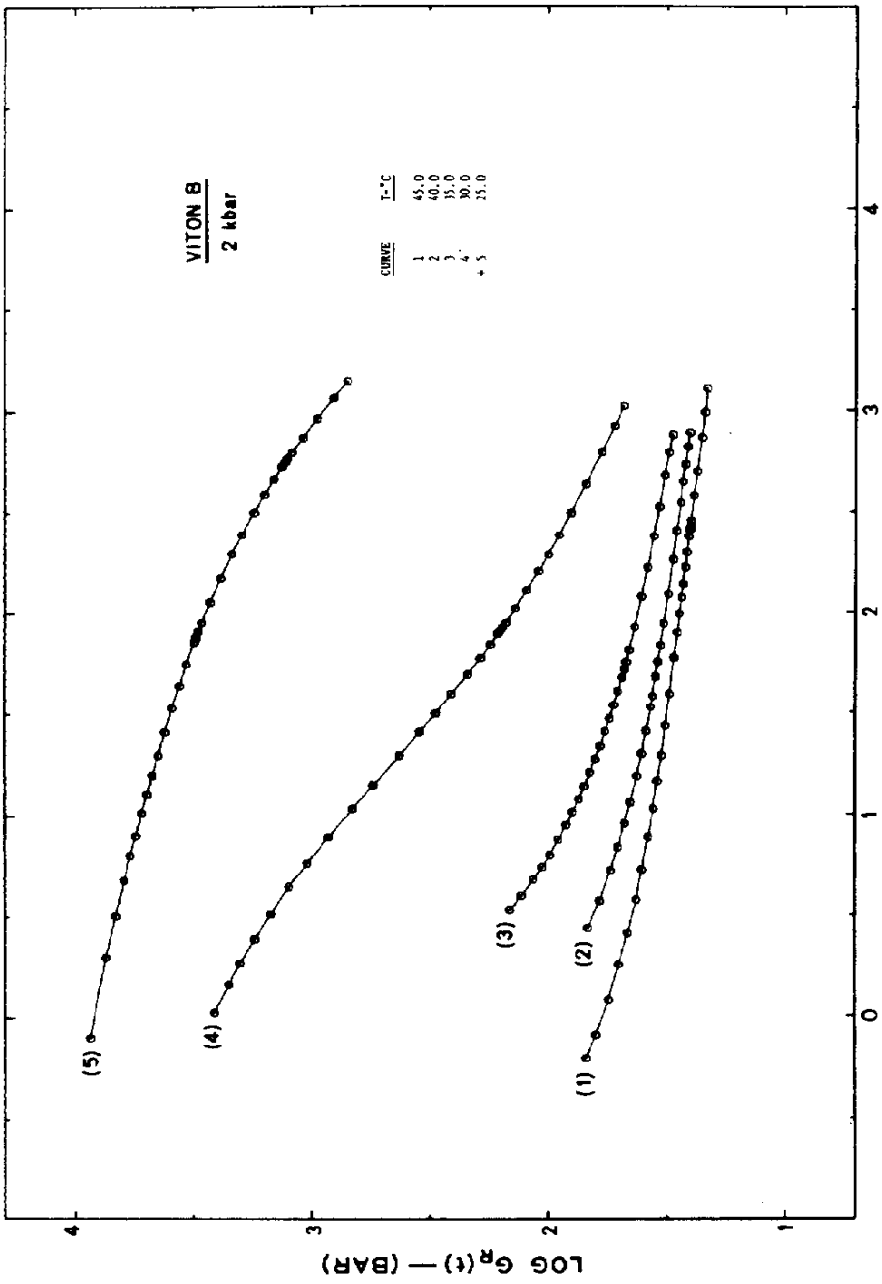

Fig. 10. Viton B: shear modulus, $G_R(t)$, at P = 2,000 bar and temperatures as indicated.

(B), and (C) in Figure 11 are derived from the segments shown in Figures 4, 5, and 6. They represent the behavior of Hypalon 40 at 25°C at the pressures of 1, 1000, and 2000 bars, respectively. The empirical shift distances, log $a_{T,1}$, log $a_{T,1000}$, and log $a_{T,2000}$ as functions of the temperature, T, are represented by the circles in the insert. Curve (A) is repeated in Figure 12 for comparison with curve (D) derived from the segments shown in Figure 3. The insert displays the empirical shift distances, log $a_{25,P}$, employed in constructing curve (D). Taking the appropriate shift distances from the insert in Figure 12, curves (A), (B), and (C) may be brought into superposition with each other.

Curves (A) and (D) contain the same information: the time dependence of the shear relaxation modulus over 12 decades of time at 25.0°C and 1.0 bar (i.e. atmospheric) pressure. Their coincidence in the rubbery and in most of the transition region indicates the material to be piezo- and thermorheologically simple. The slight difference in the glassy region is not surprising. Glasses formed by the application of pressure are generally found to be denser than those formed by lowering the temperature[21,25] and we expect the denser glass to display the greater shear modulus.

The data on Viton B are treated analogously. The mastercurves are displayed on Figures 13 and 14. Curves (A), (B), and (C) are constructed from the segments shown in Figures 8, 9, and 10, respectively, and curve (D) from those displayed in Figure 7. The shift distances are again shown in the inserts. Comparison of Figures 12 and 14 demonstrates that the effect of pressure on Viton B is about twice that on Hypalon 40.

To effect superposition it was necessary, in some cases, to apply small vertical shifts in addition to those demanded by eq. (5). These vertical shifts were required only in the upper transition and glassy region. We suspect that they reflect, in a manner which is not clear at this time, both the inadequacy of eq. (5) in these regions and the consequences of the fact that eq. (7) does not represent the exact conversion of the tensile to the shear relaxation modulus. These shifts, which we designate by ΔG_c, are shown in Figure 15 for Hypalon 40 and in Figure 16 for Viton B. They are small on the logarithmic scale, never exceeding ± 0.24 units.

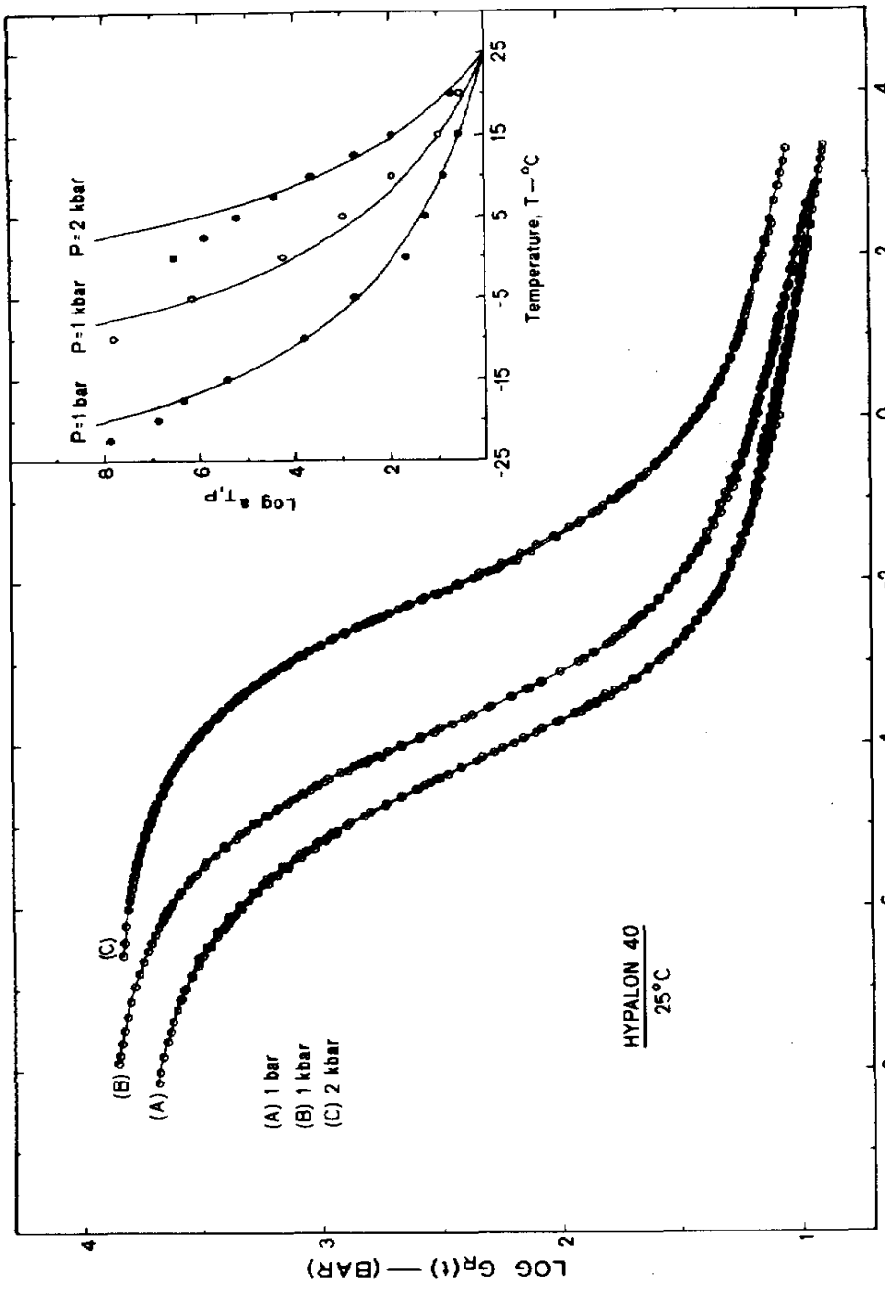

Fig. 11. Hypalon 40: mastercurves of shear modulus, $G_R(t)$, reduced by shift factors shown in insert.

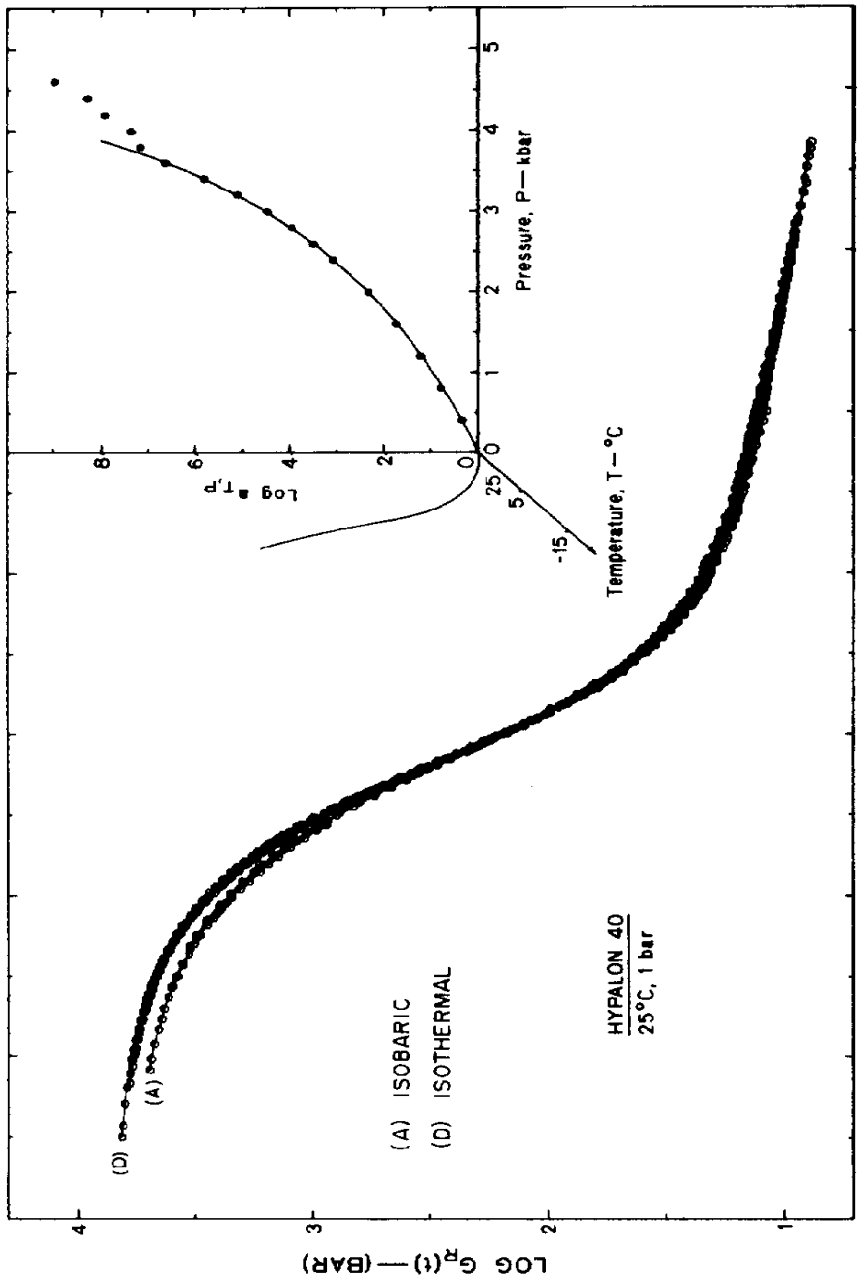

Fig. 12. Hypalon 40: mastercurves of shear modulus, $G_R(t)$, reduced by shift factors shown in the insert (D) and the Figure 11 insert (A).

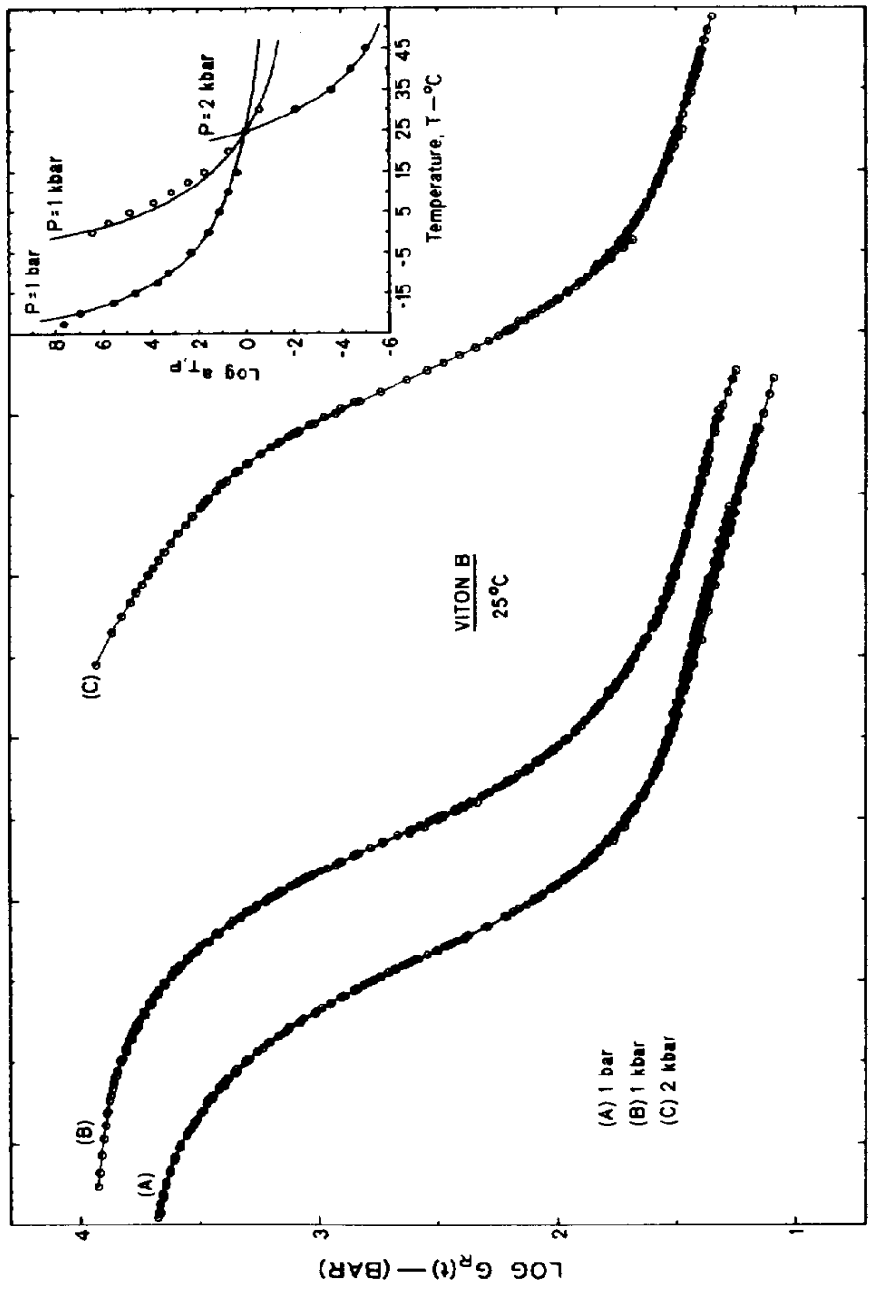

Fig. 13. Viton B: mastercurves of shear modulus, $G_R(t)$, reduced by shift factors shown in insert.

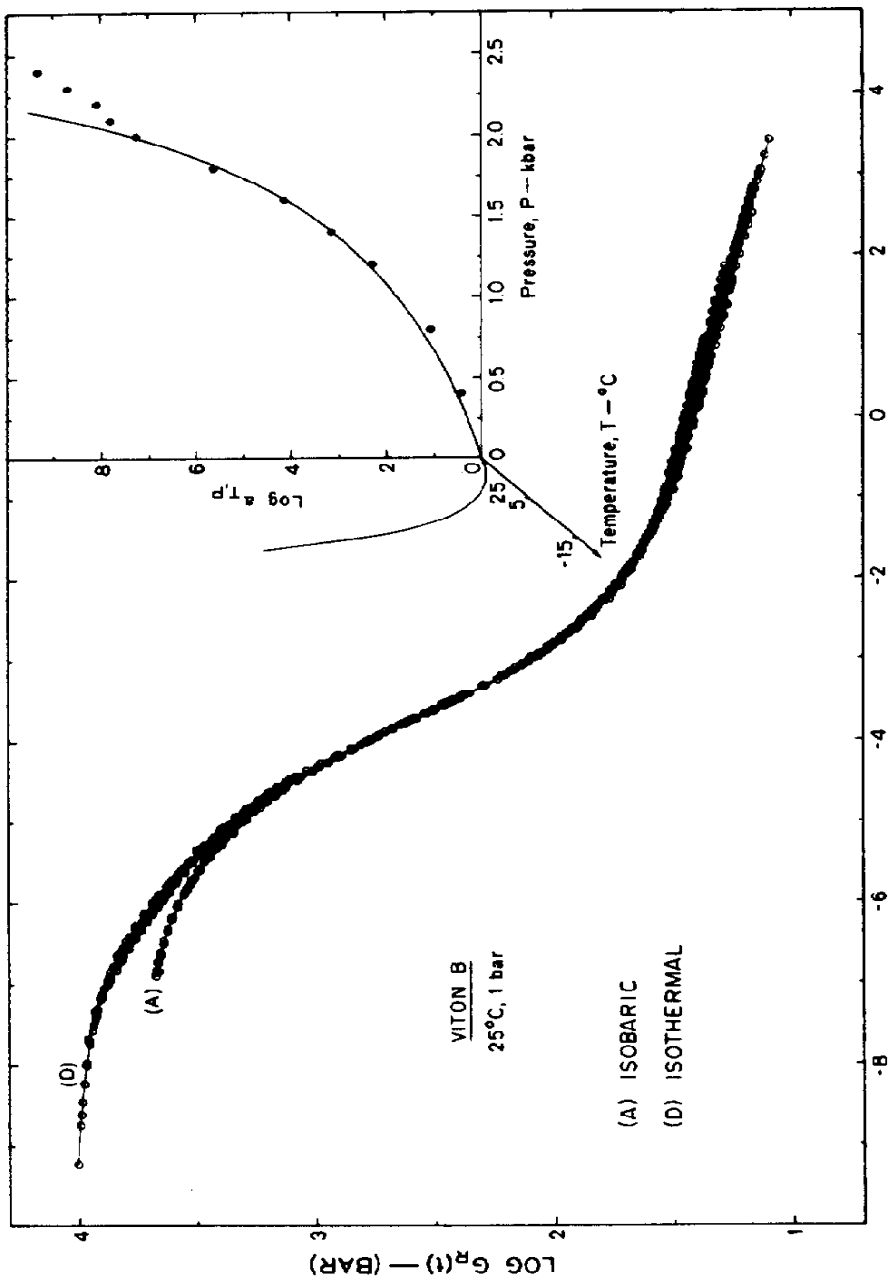

Fig. 14. Viton B: mastercurves of the shear modulus, $G_R(t)$, reduced by shift factors shown in the insert (D) and the Figure 13 insert (A).

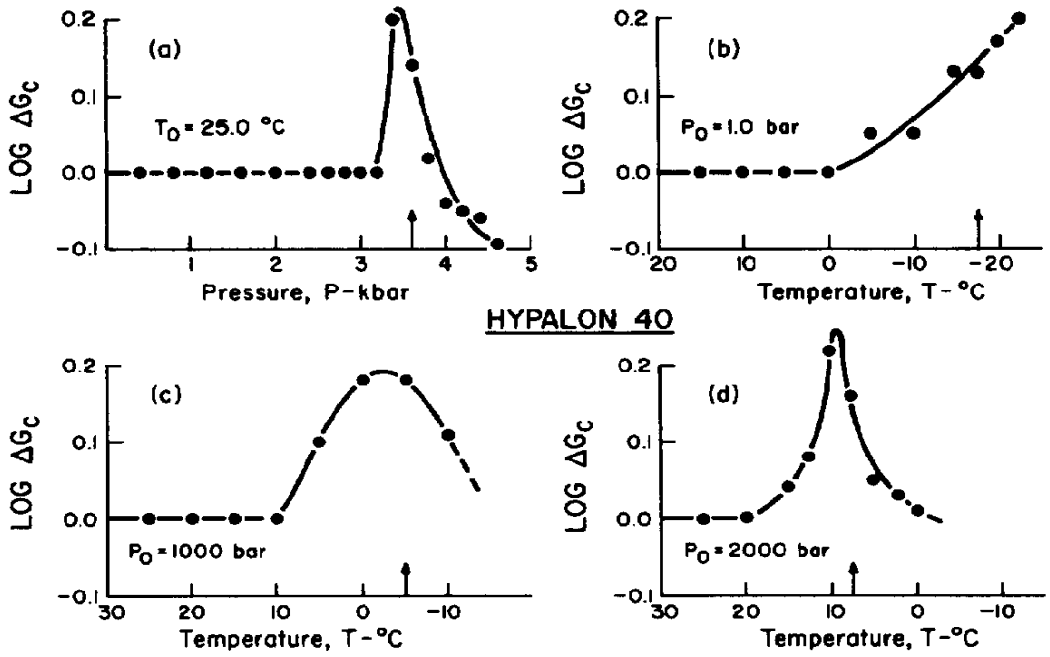

Fig. 15. Hypalon 40: vertical shifts, log ΔG_c, incorporated in data reduction; arrows indicated onset of glassy behavior.

The vertical shift factors, ΔG_c, are already contained in Figures 3 to 10. For the purposes of these figures, therefore, eq. (5) should be interpreted as

$$G_R(t) = G(t)(T_0\rho_0^0/T\rho)\ \Delta G_c. \tag{9}$$

The plus sign (+) in these figures indicates the first segment to which an additional shift, log ΔG_c, was applied. The arrows in the figures displaying the data segments indicate the pressure or temperature at which the shift factors, log $a_{T,P}$, deviate from the solid lines in the inserts in Figures 11–14. This point, although not the glass transition, T_g, as defined in the classical sense (i.e. by volumetric measurements), may be thought of as the onset of glassy behavior and will be referred to here as the inflection temperature, T_i. It is undoubtedly closely related to T_g. The data points in Figures 15 and 16 seem to lie on smooth curves displaying maxima in the vicinity of T_i.

It should be noted that the empirical vertical shifts are not completely arbitrary. In the region where the vertical shifts were ap-

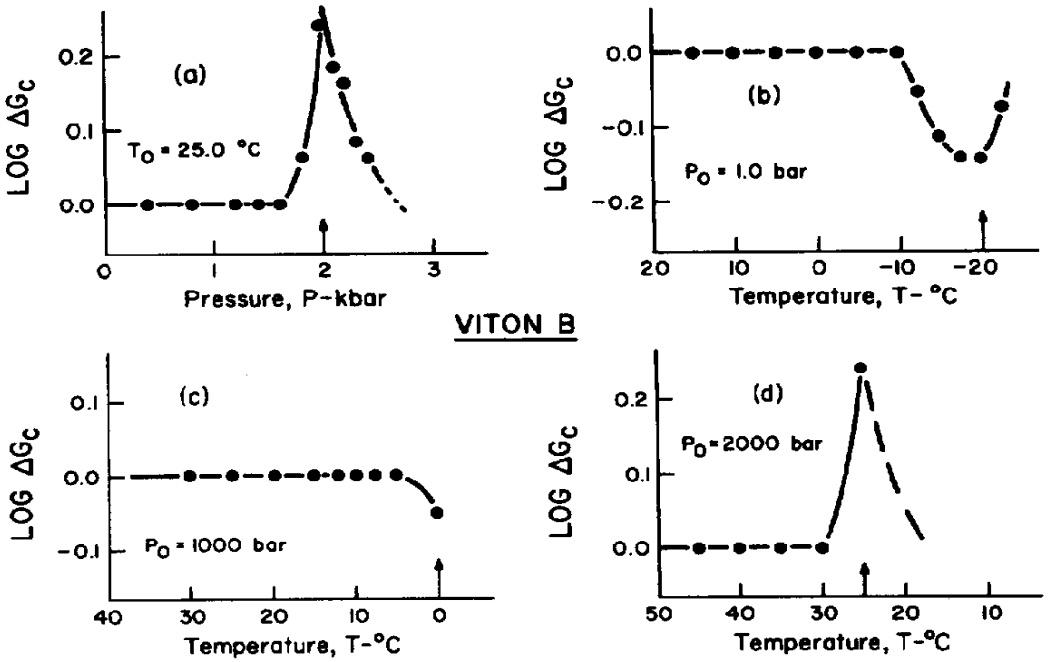

Fig. 16. Viton: vertical shifts, log ΔG_c, incorporated in data reduction; arrows indicated onset of glassy behavior.

plied, the curvature of the isothermal–isobaric data segments was such that both the vertical and the horizontal shifts were unambiguous. Furthermore, since two mastercurves are to be constructed, one from time-temperature superpositioning and a second from time-pressure superpositioning, the shifting procedure must be consistent, otherwise the two master curves will be different.

The empirical vertical shifts applied to the two materials are quite different. Those for Hypalon 40 are positive in all cases. Those for Viton B resulting from reducing the pressure data exhibit a maximum, whereas the shifts resulting from shifting the temperature data exhibit a minimum except at the higher pressures. The time-temperature data at the elevated pressures exhibit hardly any shifts at all. Thus the vertical shifts appear to be internally consistent.

The measurements on Neoprene WB are displayed in Figure 17. Data were obtained at different pressures at 25°C only.

Compressibility measurements by Weir,[19] when plotted in terms of the bulk modulus, and measurements of the tensile modulus by Patterson,[3] both showed the glass transition in Neoprene to occur at

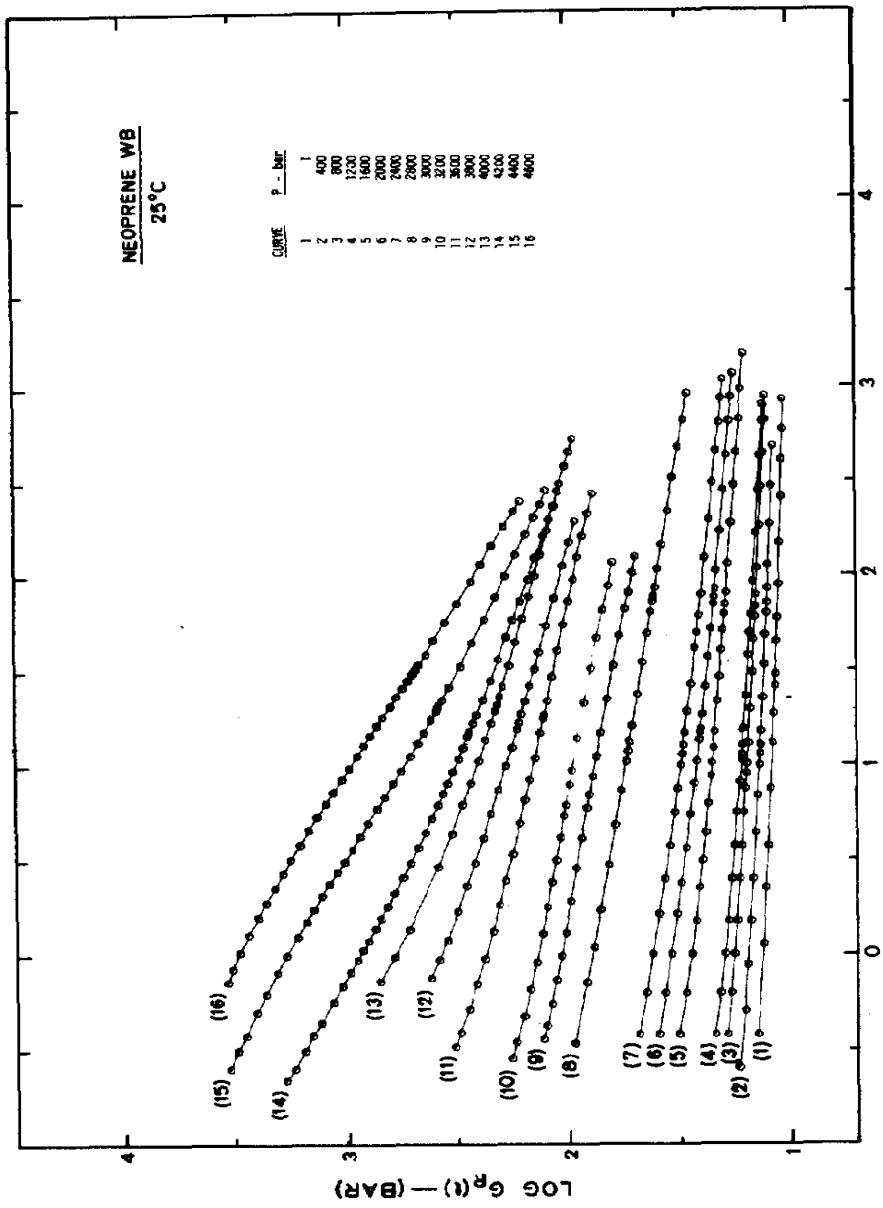

Fig. 17. Neoprene WB: shear modulus, $G_R(t)$, at $T = 25.0°C$ and pressures as indicated.

approximately 3.6 kbar pressure at 25°C. The relaxation curves in Figure 17 seem to indicate that 4.6 kbar pressure still has not induced glassy behavior. However, the initial portions of the curves at the highest pressures tend to bend over indicating the onset of glassy response.

The isothermal–isobaric data segments did not superpose well in the upper transition region. This is seen in the mastercurve shown in Figure 18. The reason for this partial lack of superposition is not clear. The shift distances, log a_P, are again plotted as functions of the pressure, P, in the insert in Figure 18.

The data on Neoprene WB are interesting because of the high percentage of filler which this material contains. The behavior of a highly filled elastomer typically deviates from that of the pure elastomer in two major ways: (1) the entire master curve is shifted to higher moduli and to somewhat longer times; and (2) non-linear stress-strain behavior is observed at much lower strains. The modulus enhancement can be seen by comparing Figure 17 with Figures 12 and 14.

The results on EPDM are given in Figures 19 and 20. Here, no vertical shift was applied to the segments ($\Delta G_c \equiv 0$) since the data would not superpose even in the rubber region. Figure 19 shows the results of measurements at 25.0°C as a function of pressure. The inability to apply time-pressure superposition to the segments is exhibited by the extreme downward curvature of the ends of the segments, and is particularly evidenced in segments (1) to (4). The lack of superposition is again found for the measurements at 1.0 bar as a function of temperature reported in Figure 20. These segments display similar behavior to the segments measured as a function of pressure. In both cases, the relaxation times are affected differently by either a change in temperature, or a change in pressure. Lack of time-temperature superposition in EPDM has been noted previously and has been attributed to crystallization.[37] Blockiness could also contribute.

We remark that, in shifting the usual isobaric temperature segments obtained at atmospheric pressure, one is commonly guided by the WLF equation derived from data in the transition region because in the rubbery region the segments are usually too flat to allow unambiguous shifting. By contrast, in constructing our master curves we let ourselves be guided by requiring that the isobaric and the iso-

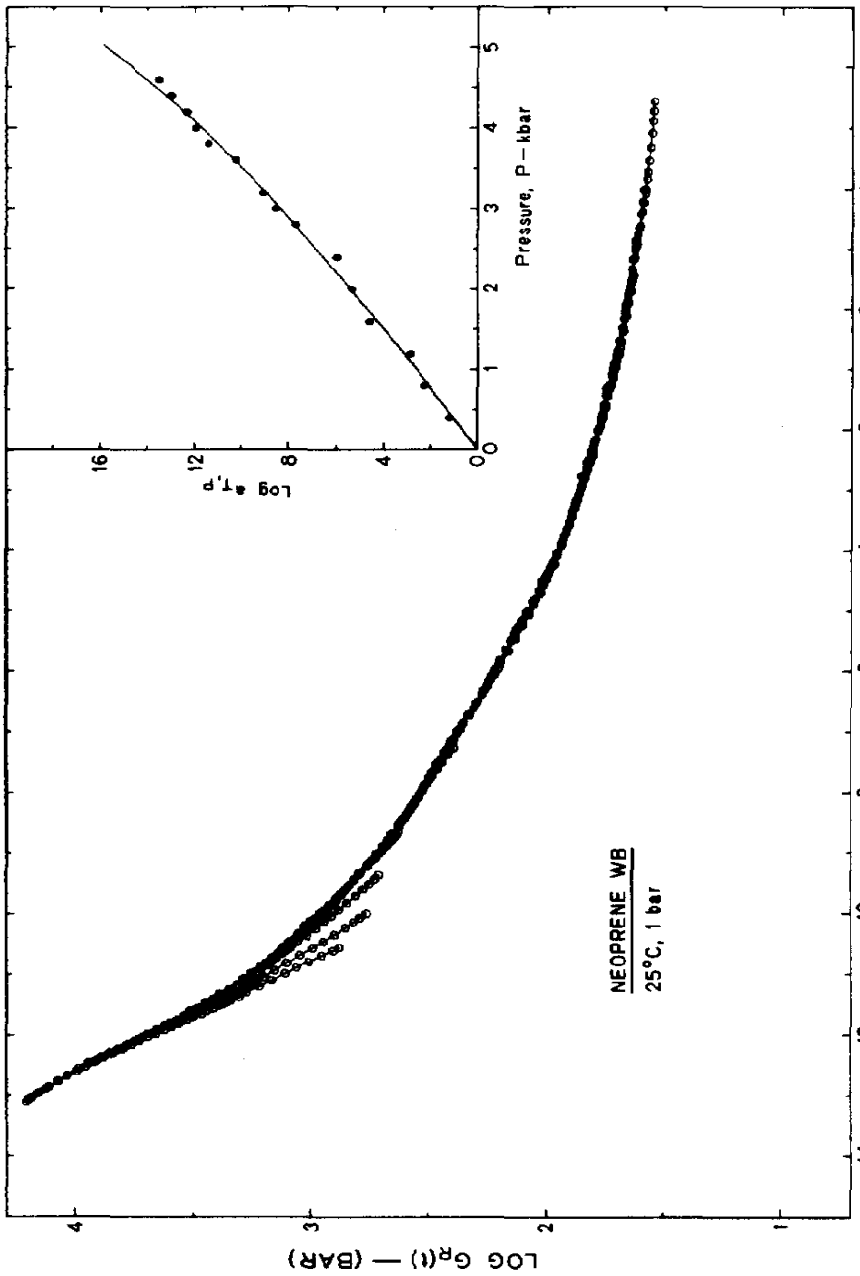

Fig. 18. Neoprene WB: mastercurve of shear modulus, $G_R(t)$, reduced by shiftf actors shown in insert.

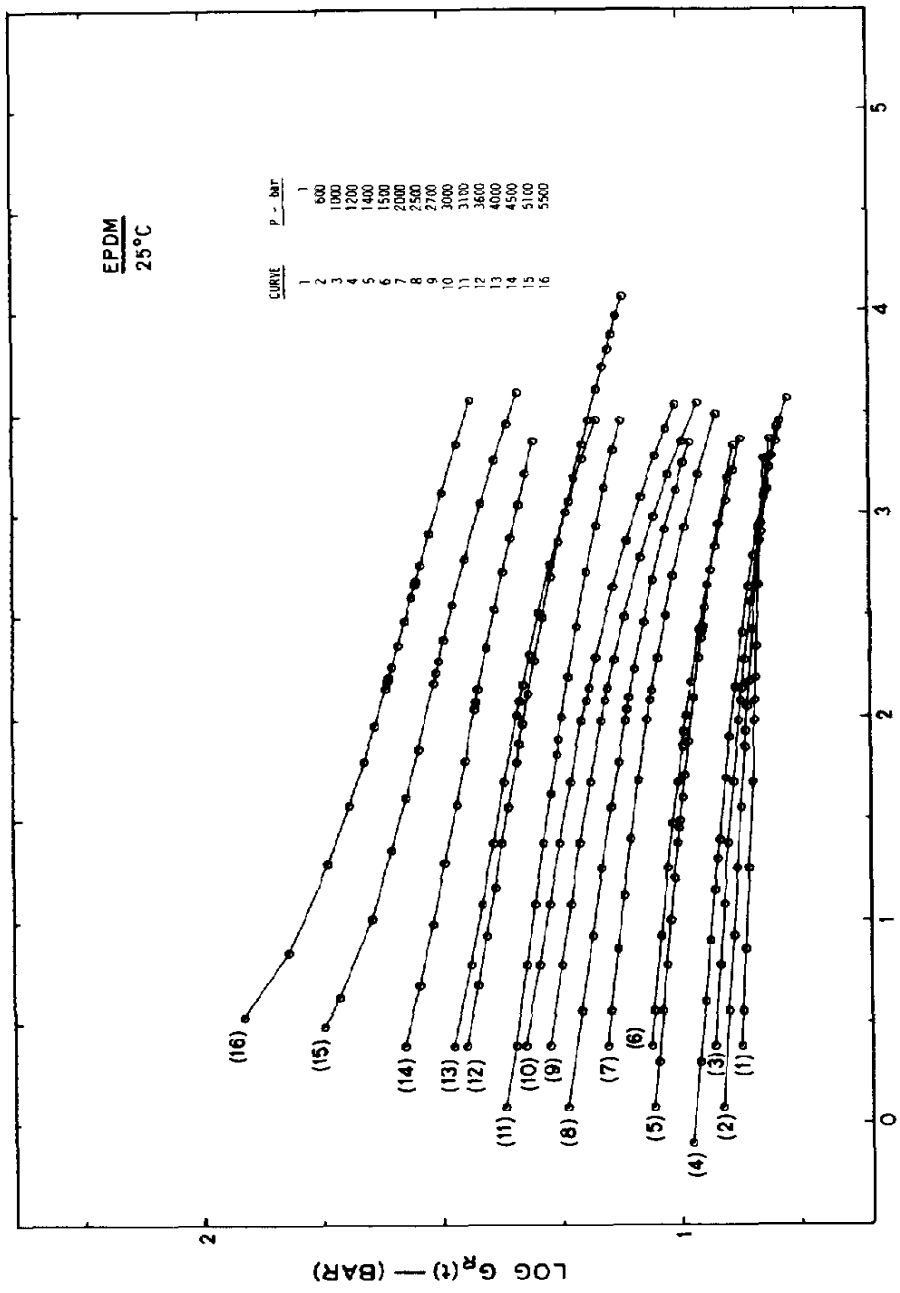

Fig. 19. EPDM: shear modulus, $G_R(t)$, at $T = 25.0°C$ and pressures as indicated.

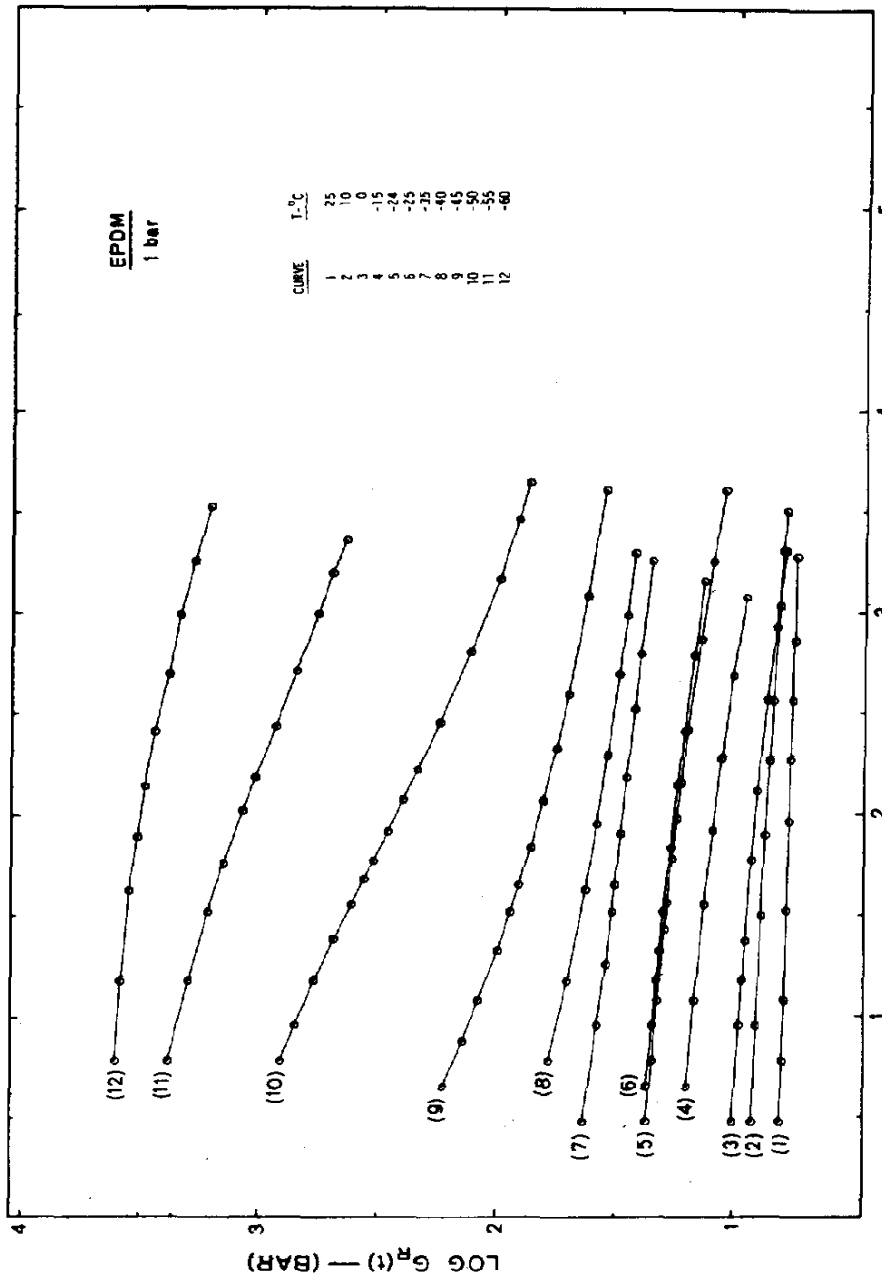

Fig. 20. EDPM: shear modulus, $G_R(t)$, at P = 1.0 bar and temperatures as indicated.

thermal master curves coincide in this region It is possible that the effect of temperature and pressure on entanglements, whose contribution would show up in this region, is different. However, in the absence of any information on this point we followed the course which seemed most expedient to us.

DISCUSSION

The data presented in the preceding section demonstrate that Hypalon 40, Viton B, and Neoprene WB (partially) are piezorheologically simple materials. In such materials the effect of time and pressure superpose, i.e.

$$\frac{\tau_i(P)}{\tau_i(P_0)} = a_{P_0}(P) = a_P, \tag{10}$$

where $\tau_i(P)$ is the ith relaxation time at pressure P, $\tau_i(P_0)$ is the same relaxation time at the reference pressure P_0, and $a_{P_0}(P)$ is a function of P for a given reference pressure. The full symbol is customarily abbreviated by a_P. For a material to be piezorheologically simple, eq. (10) must be valid for all relaxation times. Empirically determined shift distances, log a_P, plotted against the pressure, P, appear to lie on smooth curves as shown in the inserts in Figures 12, 14, and 18. However, only the shift distances obtained on Neoprene WB could be moderately well described by eq. (2). Equation (1) failed to describe any of the results. This equation was developed by Ferry and Stratton[7] on the basis of the free volume approach. The authors assumed the compressibility of the free volume to be independent of pressure. We shall show that the incorporation of the correct pressure dependence of the compressibility leads to a new equation which very satisfactorily describes the pressure dependence of the mechanical response of Hypalon 40, Viton B, Neoprene WB, and the published data of Zosel[11] on poly(vinyl chloride).

We shall derive the new equation for the general case of combined temperature and pressure effects. In doing so we will follow the free volume approach. There is some indication that a better description might be obtained using the excess entropy or excess enthalpy.[15,38–40] The matter does not appear to have been definitely settled at this time.

Theory

We consider that the general shift factor, $a_{T,P}$, can be related to the steady-flow viscosity, η, at the temperature T and the pressure P by

$$a_{T,P} = \eta/\eta_0, \tag{11}$$

where η_0 is the steady-flow viscosity in the reference state. In principle, the ratio on the right of eq. (11) should be multiplied by the same factor, $T_0\rho_0{}^0/T\rho$, which appeared in eq. (5). This factor, however, is commonly omitted from consideration.[5]

We assume that the temperature and pressure dependence of the steady-flow viscosity can be described by the temperature and pressure dependence of the free volume through the Doolittle equation,[41]

$$\eta = A \exp (BV_\phi/V_f), \tag{12}$$

where V_ϕ and V_f are the occupied and free volumes, respectively, and A and B are unspecified parameters. The sum of V_ϕ and V_f is the total volume, V. We combine the Doolittle equation with eq. (11) to obtain

$$\ln a_{T,P} = B\left[\frac{1}{f(T, P)} - \frac{1}{f(T_0, P_0)}\right], \tag{13}$$

where $f(T, P)$ is the fractional free volume at temperature T and pressure P.

$$f(T, P) = V_f/V \approx V_f/V_\phi. \tag{14}$$

The second equation on the right follows because $V_f \ll V_\phi$. We now turn our attention to the effect of temperature and pressure on the fractional free volume, $f(T, P)$.

Since we are interested in the change in the fractional free volume with pressure and temperature, we differentiate f to obtain

$$df = \left(\frac{\partial f}{\partial P}\right)_T dP + \left(\frac{\partial f}{\partial T}\right)_P dT, \tag{15}$$

and then integrate eq. (15), choosing the path shown below:

$$\int_{T_0,P_0}^{T,P} df = \int_{P_0}^{P} \left(\frac{\partial f}{\partial P}\right)_{T_0} dP + \int_{T_0}^{T} \left(\frac{\partial f}{\partial T}\right)_P dT. \tag{16}$$

As will be shown later, the choice of this path requires that we know the pressure dependence of the expansivity. Had we chosen the alternative path, integrating $(\partial f/\partial T)_{P_0}$ from T_0 to T, and $(\partial f/\partial P)_T$ from P_0 to P, we would have to consider the temperature dependence of the compressibility. There is no difference in principle but the first path is slightly simpler, particularly since it is not known whether the parameter k in eq. (8a) is indeed independent of temperature.

We now consider the partial differentials in eq. (16). Since $V_f = V - V_\phi$, differentiation with respect to temperature at constant pressure yields

$$\frac{1}{V}\left(\frac{\partial V_f}{\partial T}\right)_P = \frac{1}{V}\left(\frac{\partial V}{\partial T}\right)_P - \frac{1}{V}\left(\frac{\partial V_\phi}{\partial T}\right)_P . \tag{17}$$

We write

$$\alpha_f = \alpha_r - \alpha_\phi, \tag{18}$$

where, by the definition of the volume expansivity,

$$\alpha_P = \frac{1}{V}\left(\frac{\partial V}{\partial T}\right)_P . \tag{19}$$

α_f, α_r, and α_ϕ are the isobaric expansivities of the free volume, the rubber, and the occupied volume, respectively. Differentiation of eq. (14) with respect to temperature at constant pressure gives

$$\left(\frac{\partial f}{\partial T}\right)_P = \frac{1}{V}\left(\frac{\partial V_f}{\partial T}\right)_P - \frac{V_f}{V^2}\left(\frac{\partial V}{\partial T}\right)_P = \alpha_f - f\alpha_r. \tag{20}$$

Neglecting $f\alpha_r$ then leads to

$$\left(\frac{\partial f}{\partial T}\right)_P \simeq \frac{1}{V}\left(\frac{\partial V_f}{\partial T}\right)_P = \alpha_f(P). \tag{21}$$

Defining the isothermal compressibility in the usual way as

$$\kappa_T = -\frac{1}{V}\left(\frac{\partial V}{\partial P}\right)_T , \tag{22}$$

differentiation of eq. (14) with respect to pressure at constant temperature yields

$$\kappa_f = \kappa_r - \kappa_\phi, \tag{23}$$

where κ_f, κ_r, and κ_ϕ are the compressibilities of the free volume, the rubber, and the occupied volume, respectively. Differentiating eq. (14) similarly leads to

$$\left(\frac{\partial f}{\partial P}\right)_{T_0} \simeq \frac{1}{V}\left(\frac{\partial V_f}{\partial P}\right)_{T_0} = -\kappa_f(T_0). \tag{24}$$

We may now substitute eqs. (21) and (24) into eq. (16) to obtain

$$f(T, P) - f(T_0, P_0) = -\int_{P_0}^{P} \kappa_f(T_0)\, dP + \int_{T_0}^{T} \alpha_f(P)\, dT, \tag{25}$$

where $\kappa_f(T_0)$ is the compressibility of the free volume at the reference temperature, T_0, and $\alpha_f(P)$ is the expansivity of the free volume at the test pressure, P. Using eq. (23), we write the first term on the right of eq. (25) as

$$\int_{P_0}^{P} \kappa_f(T_0)\, dP = f_{T_0}(P) = \int_{P_0}^{P} \kappa_r(T_0)\, dP - \int_{P_0}^{P} \kappa_\phi(T_0)\, dP. \tag{26}$$

We will consider the indicated integration further on. For the second term we have

$$\int_{T_0}^{T} \alpha_f(P)\, dT = f_P(T) = \alpha_f(P)[T - T_0]. \tag{27}$$

This term can be integrated immediately because the temperature dependence of $\alpha_f(P)$ may be neglected.

Now, using the abbreviation

$$f_0 = f(T_0, P_0) \tag{28}$$

for the fractional free volume at the reference temperature and pressure, combining eqs. (25), (26), and (27) gives

$$f(T, P) = f_0 + f_P(T_0) - f_{T_0}(P). \tag{29}$$

Substituting eqs. (28) and (29) into eq. (13) then finally yields

$$\log a_{T,P} = -\frac{B}{2.303\, f_0}\left[\frac{f_P(T) - f_{T_0}(P)}{f_0 + f_P(T) - f_{T_0}(P)}\right], \tag{30}$$

which is our new equation for the shift distance, $\log a_{T,P}$.

If we set $P = P_0$, where P is any constant pressure, in eq. (30), we recover the WLF equation. Setting $T = T_0$ and assuming that the compressibilities do not depend on pressure, we obtain

$$f_{T_0}(P) = \kappa_f(P - P_0) \tag{31}$$

and regain the Ferry–Stratton equation. If, on the other hand, it is assumed that the fractional free volume is simply inversely proportional to the pressure,[6] i.e. that

$$f(T_0, P) = f_0 - f_{T_0}(P) = \Pi f_0/(P + \Pi), \tag{32}$$

where Π $(=\Pi' - P_0)$ is an empirical constant, then we obtain eq. (2). The difference between eqs. (2) and (30) is that we apply the inverse pressure dependence to the compressibility, not the free volume.

To apply eq. (30) we must return to the integrations indicated in eq. (25). The compressibility is the reciprocal of the bulk modulus. Hence, by eq. (8a),

$$\kappa_T = \frac{1}{K^*(T) + kP}. \tag{33}$$

Assuming that the pressure dependence of the compressibility of the occupied volume has the same form as that of the rubber, integration of eq. (25) yields

$$f_{T_0}(P) = \frac{1}{k_r} \ln \frac{K^*_r + k_r P}{K^*_r + k_r P_0} - \frac{1}{k_\phi} \ln \frac{K^*_\phi + k_\phi P}{K^*_\phi + k_\phi P_0}, \tag{34}$$

where K^*_r and K^*_ϕ are the bulk moduli of the rubber and the occupied volume, respectively, at zero pressure and at the reference temperature, T_0.

The parameters K^*_r and k_r may be obtained from volume–pressure measurements on the rubber through a fit[34] to Murnaghan's equation,

$$V = V^0 \left[\frac{K^*(T) + kP}{K^*(T) + kP_0} \right]^{-1/k}, \tag{35}$$

where V^0 is the volume at the reference pressure P_0 and the temperature T. Equation (35) was used successfully by Murnaghan[42] to fit Bridgman's data[18] on various solids and was shown to hold for

rubbers also.[34,35] It is obtained by combining eqs. (22) and (33) into

$$d \ln V = - \frac{dP}{K^*(T) + kP} \tag{36}$$

and integrating at constant temperature between the limits V^0 and P_0, and V and P, respectively.

If the compressibility is defined by

$$\beta_T = - \frac{1}{V_0} \left(\frac{\partial V}{\partial P} \right)_T, \tag{37}$$

combination with eq. (33) and integration yields the Tait equation[34,43,44]

$$V = V^0 \left[1 + \ln \left(\frac{K^*_t + k_t P}{K^*_t + k_t P_0} \right)^{-1/k_t} \right]. \tag{38}$$

This equation fits volume–pressure data on rubbers equally well.[34] The quantities K^* and K on the one hand, and K^*_t and K_t on the other, are, of course, different. Values of $f_{T_0}(P)$ calculated with either pair differ negligibly, however.

We note that, because of our choice of the path of integration in eq. (16), K_r (and K_ϕ) are to be taken at the reference temperature. Hence, eq. (34) remains valid even if k_r (and k_ϕ) should depend on temperature, as long as they were determined at the temperature chosen as reference.

Equation (31) may be recast in the more convenient form:

$$\log a_{T,P} = - \frac{c_1[T - T_0 - \theta(P)]}{c_2 + T - T_0 - \theta(P)}, \tag{39a}$$

where

$$\theta(P) = f_{T_0}(P)/\alpha_f(P) = c_3 \ln \left[\frac{1 + c_4 P}{1 + c_4 P_0} \right] - c_5 \ln \left[\frac{1 + c_6 P}{1 + c_6 P_0} \right] \tag{39b}$$

and

$$c_1 = B/2.303 f_0, \tag{40a}$$

$$c_2 = f_0/\alpha_f(P), \tag{40b}$$

$$c_3 = 1/k_r \alpha_f(P), \tag{41a}$$

$$c_4 = k_r/K^*_r, \tag{41b}$$

$$c_5 = 1/k_\phi \alpha_f(P), \tag{41c}$$

$$c_6 = k_\phi/K^*_\phi. \tag{41d}$$

At the reference pressure, $\theta(P) = 0$ and eq. (39a) reduces to the WLF equation containing only the "temperature parameters" c_1 and c_2. Thus, the form of the WLF equation is preserved for isobaric measurements at any pressure However, c_1 and c_2 are functions of pressure because

$$f(T_0, P) = f_0 - f_{T_0}(P) \tag{42}$$

by eq. (29), and $\alpha_f(P)$ must also be taken at the test pressure P. To obtain the pressure dependence of the thermal expansivity at the reference temperature, we set $P_0 = 0$ in eq. (35). This gives

$$V = V^*[1 + kP/K^*(T)]^{-1/k}, \tag{43}$$

where V^* is the volume at zero pressure and temperature T. We then differentiate this expression for V with respect to T at constant pressure, making use of eq. (8b). Provided that k is independent of temperature, this yields

$$\frac{1}{V}\left(\frac{\partial V}{\partial T}\right)_P = \frac{1}{V^*}\left(\frac{\partial V^*}{\partial T}\right)_P - \frac{m\alpha^* P}{K^*(T) + kP}. \tag{44}$$

Using eq. (19) we then obtain the pressure dependence of the volume expansivity of the rubber at the reference temperature as[36]

$$\alpha_r(P) = \alpha^*_r\left(1 - \frac{mP}{K^*_r + k_r P}\right), \tag{45}$$

where α^*_r is the expansivity of the rubber at zero pressure. From eq. (45) we derive an expression for the pressure dependence of the expansivity of the free volume by again assuming that the pressure dependence of the occupied volume follows an equation of the same form as that of the rubber, containing the same parameter m. Thus, we write

$$\alpha_\phi(P) = \alpha^*_\phi\left(1 - \frac{mP}{K^*_\phi + k_\phi P}\right). \tag{46}$$

Blatz has shown[36] that the same m holds for the rubber and the glass. Hence, our assumption appears reasonable. Using eq. (18) we obtain

$$\alpha_f(P) = \alpha^*_f\left(1 - \frac{mP}{K^*_r + k_r P}\right) - \alpha^*_\phi mP\left(\frac{1}{K^*_r + k_r P} - \frac{1}{K^*_\phi + k_\phi P}\right), \tag{47}$$

which we have cast in this particular form for convenience later on.

The free volume interpretation of the "temperature parameters" c_1 and c_2 describes them in terms of three unknowns, B, f_0, and $\alpha(P)$. The fractional free volume in the reference state can therefore be obtained from measurements of c_1 and c_2 at atmospheric pressure only if it is assumed either that B is unity or that $\alpha_f = \Delta\alpha = \alpha_r - \alpha_g$. There is no independent experimental evidence for the first assumption. The second requires, in view of eq. (18), that $\alpha_\phi = \alpha_g$. In explaining crazing phenomena in polypropylene in a nitrogen environment, Peterlin[45] assumes that the fractional free volume in the glassy state is not constant but proportional to the absolute temperature. From this one infers that α_g must be larger than α_ϕ.

This vexing ambiguity is at once removed, at least in principle, by the determination of the "pressure parameters" c_4 through c_6 in isothermal measurements as function of pressure. For such measurements we have

$$\log a_{T_0,P} = \frac{c_1\theta(P)/c_3}{c_2/c_3 - \theta(P)/c_3}, \tag{48}$$

because c_3 now scales the other parameters and consequently must be divided out. We then have

$$c_2/c_3 = f_0k_r, \tag{49a}$$

$$c_5/c_3 = k_rk_\phi. \tag{49b}$$

Furthermore, c_4 is known because K^*_r and k_r can be determined in a separate independent experiment. Hence, we have four equations, (40a), (41d), (49a), and (49b), for the four unknowns, B, f_0, k_ϕ, and K^*_ϕ. If, in addition, isobaric measurements are made at atmospheric pressure, α_f can be obtained from eq. (40b) and, if α_r is determined in a separate independent measurement, α_ϕ may also be found, using eq. (18).

Hence, we conclude that by combining isothermal measurements of the response functions of polymers at different pressures with the usual isobaric ones at atmospheric pressure all the molecular parameters, B, f_0, α_f, k_ϕ, and K^*_ϕ, may be determined unambiguously, provided always that the experiments can be made with sufficient accuracy.

Applications

We are now ready to consider eq. (39) in the light of our experimental data. The applicability of eq. (39) can, of course, be verified

by means of the data without any attempt at a molecular interpretation of the c's. In such an interpretation we are hampered by the absence of direct measurements of α_r, K^*_r, k_r, and m on the materials we have investigated. We thought it worthwhile, however, to estimate the molecular papameters by means of informed guesses regarding the missing parameters. We emphasize that these estimates must be considered with caution. They can be refined when direct measurements of the expansivity and compressibility parameters of the rubbers become available.

We take the results on Neoprene WB first. These data were obtained at 25°C at fifteen pressures between 1 and 4600 bars. As with the other materials to be discussed later, atmospheric pressure (1 bar) was taken as the reference pressure. The pressure parameters, c_1, c_2/c_3, c_4, c_5/c_3, and c_6 were obtained from the empirical shift distances, log $a_{T_0,P}$, plotted in the insert of Figure 18, through a non-linear least squares fit to eq. (39). The solid line in the insert represents the equation with the following numerical values of the parameters: $c_1 = 7.94$, $c_2/c_3 = 0.1940$, $c_4 = 0.4695$, $c_5/c_3 = 0.9248$, and $c_6 = 0.4409$. The fit is very satisfactory. We calculated the molecular parameters by assuming that the value of $k_r = 10.8$ as determined from the data of Weir[19] for an unfilled neoprene would apply to our filled material as well. In fact, the value of $c_3 = 1/10.8$ was held fixed during the least-squares fitting. The calculated parameters are assembled in Table I. They depend on the chosen value of k_r and this is indicated by underscoring this value in the table. It is interesting that the value of K^*_r is the same as that which we determined from Weir's[19] data on his unfilled neoprene. The compressibility parameters of the occupied volume are larger than those of the rubber, as expected, but not much larger. Particularly noteworthy is the finding that B is far from unity.

In the cases of Hypalon 40 and Viton B we had no ready estimate for either k_r of K^*_r. Therefore, the experimental shift distances were fitted to eq. (39), holding none of the parameters constant. The data obtained at atmospheric pressure as function of temperature and those obtained at 25°C as a function of pressure were fitted simultaneously. The resulting numerical values are: $c_1 = 2.66$, $c_2 = 60.0$, $c_3 = 152.0$, $c_4 = 0.526$, $c_5 = 105.8$, $c_6 = 0.576$ for Hypalon 40; and $c_1 = 2.24$, $c_2 = 59.4$, $c_3 = 145.6$, $c_4 = 0.402$, $c_5 = 69.4$, and $c_6 = 0.395$ for Viton B. The solid lines in the inserts of Figures 12

TABLE I
Molecular Parameters[a]

Parameter	Neoprene WB	Hypalon 40	Vitron B	PVC
B	0.329	0.230	0.175	0.608
f_0	0.0180	0.0375	0.0338	0.0401
α_f	—	6.25	5.69	—
k_r	10.8	10.5	12.1	6.0
K_r^*	23.0	20.0	30.0	22.4
k_ϕ	11.7	15.1	25.3	11.0
K_ϕ^*	26.5	26.3	64.0	41.9
m	—	2.3	4.6	—
α_r	—	(7.30)	(6.15)	—
α_ϕ	—	(1.05)	(0.49)	—
α_g	—	(4.40)	—	—

[a] Values of α_f are in 10^{-4} reciprocal degrees Celsius; values of K^* are in kbar; the other quantities are dimensionless.

and 14 and those for $P = 1.0$ bar in the inserts of Figures 11 and 13 represent eq. (39) with the above values of the c's for the isothermal and isobaric measurements, respectively. The fit is excellent. No satisfactory fit could be obtained with either eqs. (1) or (2). The deviations at low temperatures and high pressures mark the onset of the glass transition.

For both materials we have six equations, eqs. (40) and (41), for the seven unknowns: B, f_0, α_f, K^*_r, k_r, K^*_ϕ, and k_ϕ. For Hypalon 40 we calculated the molecular parameters listed in Table I by assuming the "universal" value of 20.0 kbar for K^*_r. This value also gave a satisfactory fit to the data obtained at 1 and 2 kbar pressure, respectively, which will be considered presently. For Viton B this choice yielded an unreasonably high value for α_f and did not allow a satisfactory fit to the 1 kbar and 2 kbar data. We therefore selected $K^*_r = 30.0$ as a suitable value. The underscoring in Table I again denotes those values that were introduced to allow calculation of the others in the absence of experimental values for K^*_r. We note that, in principle, the experimental determination of K^*_r is sufficient to allow the calculation of the others without ambiguity. Thus, it is not strictly necessary to know k_r also, although knowledge

of it should increase the precision with which the other parameters may be found.

For Hypalon 40, we attempted to estimate α_ϕ from α_f and the value[46] of α_r for Hypalon 20 shown in Table I. For Viton B we used the value for Viton A determined by Frensdorff.[47] Hypalon 20 and Viton A have different compositions from our materials but the expansivities are not expected to be grossly different. Because they apply to different materials, these parameters are put in parentheses in Table II. We have no values of the expansivity of the glass for Viton B or A. However, α_g for Hypalon 20 is given by Yin and Pariser.[48] It seems safe to conjucture that $\alpha_\phi < \alpha_g$ for Hypalon 40, as required by Peterlin.[45]

The practical usefulness of eq. (39) lies in its predictive power. We test this by means of the measurements which we made on Hypalon 40 and on Viton B as function of temperature at 1 kbar and 2 kbar pressure, respectively. Since these are isobaric measurements, we need the "temperature parameters" c_1 and c_2 at the pressure P. We should have

$$c_1^P = B/2.303f(T_0, P), \tag{51a}$$

$$c_2^P = f(T_0, P)/\alpha_f(P), \tag{51b}$$

where $f(T_0, P)$ and $\alpha_f(P)$ must be found from eqs. (42) and (47), respectively. Equation (47) requires knowledge of α^*_f, α^*_ϕ, and m. We used α_f for α^*_f. The difference should be negligible. Not having properly determined values of α_ϕ available, we simply omitted the second term in eq. (47). Using the values for α_ϕ listed in Table I,

TABLE II

Parameters at Elevated Pressures[a]

Material	P	$f(T_0,P)$	$\alpha_f(P)$	c_1^P	c_2^P
Hypalon 40	0.001	0.0375	6.25	2.64	56.0
	1	0.0274	5.78	3.64	47.4
	2	0.0199	5.56	5.01	35.8
Viton B	0.001	0.0338	5.69	2.24	59.4
	1	0.0190	5.07	4.00	37.4
	2	0.0079	4.73	9.61	16.7

[a] Pressures are in kbar; $\alpha_f(P)$ in 10^{-4} reciprocal degrees Celsius; and c_2 in °C.

it can be ascertained that this small correction is negligible. Suitable values of m were found by trial and error. We then calculated c_1^P and c_2^P at 1 kbar and 2 kbar pressure, respectively, using the parameters listed in Table I. The values of $f(T_0, P)$, $\alpha_f(P)$, c_1^P, and c_2^P thus obtained are tabulated in Table II and compared with those at the reference pressure of 0.001 kbar.

The solid lines for $P = 1$ and $P = 2$ kbar in the inserts in Figures 11 and 13 show the fit of eq. (39) with $\theta(P) = 0$ and c_1^P and c_2^P as listed in Table II. The fit is the more remarkable because of the assumptions that had to be made to obtain the molecular parameters at atmospheric pressure. It lends confidence to these assumptions and displays the predictive power of eq. (39).

With pressure as an additional variable, the WLF line in the shift distance-temperature plane now becomes a surface in shift distance-temperature-pressure space. The three-dimensional character of eq. (33) is displayed in Figures 21 and 22 for Hypalon 40 and Viton B, respectively. The glassy behavior is mostly conjectural since little information was obtained in this region. It is seen that the temperature at which the behavior becomes glassy occurs at a constant value of log $a_{T,P}$. This is consistent with the experimental results and implies that time-pressure superposition yields the same results as time-temperature superposition.

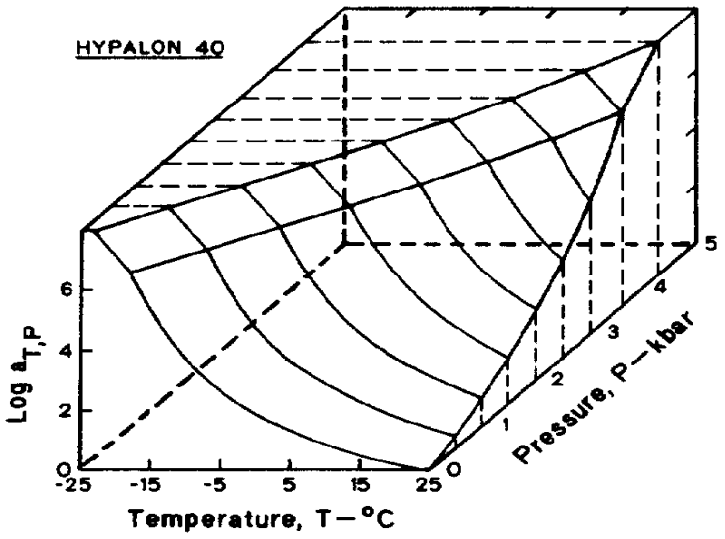

Fig. 21. Hypalon 40: shift factors, log $a_{T,P}$; dependence on temperature and pressure.

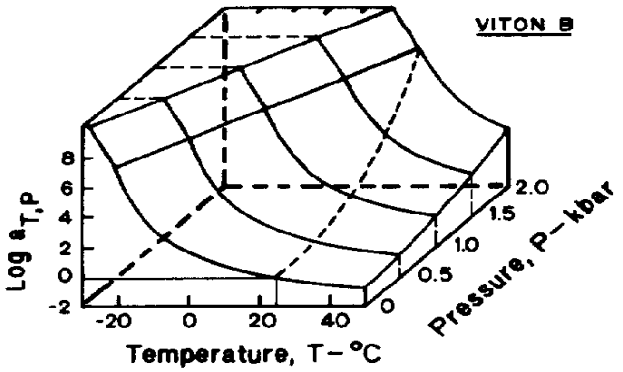

Fig. 22. Viton B: shift factors, log $a_{T,P}$; dependence on temperature and pressure.

The intersection of the regions of rubbery and glassy behavior is a straight line for Viton B and is nearly so for Hypalon 40. This implies that dT_g/dP is nearly constant for these materials over this range of temperature and pressure. The value for Viton B is about one and a half times that for Hypalon 40. This is in accordance with the observed behavior. As shown by a comparison of Figures 11 and 13, pressure has about one and a half to two times the effect on Viton B than on Hypalon 40.

Finally, we reexamined the data of Zosel[11] on PVC. Fitting the log $a_{T_0,P}$ data contained in *his* Figure 22 to *our* eq. (39) gave the following numerical values: $c_1 = 6.58$, $c_2/c_3 = 0.2407$, $c_4 = 0.268$, $c_5/c_3 = 0.5467$, and $c_6 = 0.262$. We obtained K^*_r from the work of Heydemann and Guicking[49] and estimated k_r from their measurements of $\alpha_r(P)$. The appropriate values are listed in Table I. K^*_r and k_r were held constant during the fitting procedure. The fit is shown in Figure 23. We note again that Zosel could not obtain a satisfactory fit with either eq. (1) or (2).

CONCLUSIONS

Equation (39) satisfactorily describes the pressure dependence of the mechanical properties of the materials examined here. There is no reason to believe that it should not be applicable to other piezorheologically simple materials. Once the necessary molecular parameters are known, eq. (39) may be used to predict the mechanical properties at any other pressure if they are known at atmospheric pressure.

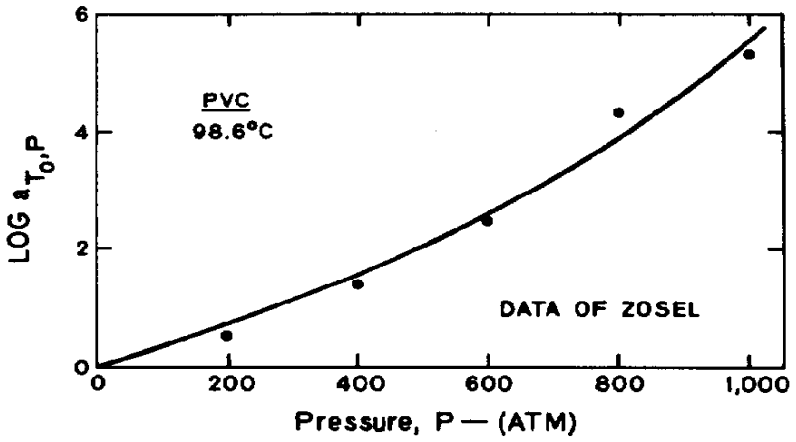

Fig. 23. PVC (data of Zosel); shift factors, log a_P, as a function of pressure.

Combination of isobaric measurements with isothermal measurements at atmospheric pressure allows the parameters B, f_0, α_ϕ, k_ϕ, and K^*_ϕ to be determined if α_r, k_r, and K^*_r have been obtained in separate experiments, provided sufficient accuracy can be reached. The ambiguity inherent in the determination of B, f_0, and α_ϕ from the usual measurements at atmospheric pressure is thus removed.

It appears fairly certain that $B \neq 1$, as commonly assumed. This, coupled with the additional support we have presented that $\alpha_f \neq \Delta\alpha = \alpha_r - \alpha_g$, forces a reexamination of literature data on f_0 and encourages experimentation on the lines we have presented here.

APPENDIX I

Compounding Recipes[29]

Hypalon 40	100
AC, PE 617A	5
SRF black	4
Epon 828	15
MBTS	0.5
Tetrone A	1.5
DOTG	0.25
Cure: 30 min. at 307°F	

Neoprene WB	50
Neoprene WRT	50
Neozone A	2
stearic acid	0.5
MT black	100
hard clay	25
LPO	12
red lead	20
Thionex	1
sulfur	1
Cure: 20 min. at 307°F	

Viton B	100
M_gO	15
MT black	20
LD-214	3
Cure: 30 min.	at 300°F
1 hr	at 212°F
1 hr	250°F
1 hr	300°F
1 hr	350°F
24 hr	400°F

APPENDIX II

Conversion of $E(t)$ to $G(t)$

We discuss here the derivation of eq. (7). For a linear viscoelastic material the constants E, G, and K in eq. (6) must be replaced by their Carson transforms (the s-multiplied Laplace transforms). For $\bar{G}(s)$, eq. (6) yields

$$\bar{G}(s) = \frac{3\bar{K}(s)\bar{E}(s)}{9\bar{K}(s) - \bar{E}(s)} . \tag{52}$$

Equation (52) may be simplified by assuming that the time dependence of the bulk modulus $K(t)$ is negligible compared to the time dependence of $G(t)$. This assumption is based on the work of McKinney, Belcher, and Marvin[39,40] who showed that $B'(\omega)$, the bulk storage compliance, increases by a factor of about two from glassy to rubbery behavior, whereas $J'(\omega)$, the shear storage compliance, generally increases by three to four orders of magnitude. Assuming the bulk modulus to be a constant with respect to time, we have $\bar{K}(s) = K/s$ and eq. (52) may be rewritten as

$$\bar{G}(s) = \frac{\bar{E}(s)}{3[1 - s\bar{E}(s)/9K]} , \tag{53}$$

where $K = K(T, P)$ is given by eqs. (8a) and (8b). Equation (53) cannot be inverted exactly in the general case. Equation (7) represents an approximation whose validity we wish to examine.

We consider a simple three-parameter Maxwell model representation for both the bulk and shear modulus. We have

$$K(t) = K_e + (K_g - K_e) \exp - t/\tau_K \tag{54}$$

and

$$G(t) = G_e + (G_g - G_e) \exp - t/\tau_G, \tag{55}$$

where the subscripts e and g denote the equilibrium and glassy moduli, respectively, and the τ_K and τ_g are the relaxation times. Laplace transformation yields

$$\bar{K}(s) = \frac{K_e + K_g\tau_K s}{s(1 + \tau_K s)} \tag{56}$$

and

$$\bar{G}(s) = \frac{Ge + G_g\tau_G s}{s(1 + \tau_G s)}. \tag{57}$$

Letting, for simplicity, $\tau_K = \tau_G = \tau$, and substituting eqs. (56) and (57) into the relation

$$\bar{E}(s) = \frac{9\bar{K}(s)\bar{G}(s)}{3\bar{K}(s) + G(s)} \tag{58}$$

yields, after partial fraction decomposition and inversion of the transform,

$$E(t) = \frac{9K_eE_e}{3K_e + G_e} + \frac{9K_dG_d}{3K_d + G_d} \exp - t/\tau$$

$$+ \frac{27(K_gG_e - K_eG_g)^2}{(3K_e + G_e)(3K_d + G_d)(3K_g + G_g)} \exp - t/\mu\tau, \tag{59}$$

where

$$K_d = K_g - K_e, \tag{60}$$

$$G_d = G_g - G_e; \tag{61}$$

and

$$\mu = \frac{3K_g + G_g}{3K_e + G_e}. \tag{62}$$

Equation (59) represents the tensile relaxation modulus obtained from the bulk and shear relaxation moduli given by eqs. (54) and (55). It is interesting to note that the bulk and shear relaxation spectra here consist of single lines while the corresponding tensile relaxation spectrum is comprised of two lines.

Selecting realistic values for the parameters in eqs. (54) and (55), we may now calculate $E(t)$. When this is obtained, we may consider different ways of approximating $G(t)$ from $E(t)$ and compare them with the "true" $G(t)$ given by eq. (55). One such approximation is

$$G_1(t) = E(t)/3; \tag{63}$$

another is the inversion of eq. (53). Substituting the Laplace transform of eq. (59) into eq. (53) and inverting yields

$$G_2(t) = \frac{3KE_e}{9K - E_e} + \left[\frac{3KE_g}{9K - E_g} - \frac{3KE_e}{9K - E_e}\right] \exp - t/\lambda\tau, \tag{64}$$

where

$$\lambda = \frac{9K - E_g}{9K - E_e}. \tag{65}$$

The glassy and equilibrium tensile moduli, E_g and E_e, are obtained from eq. (6).

Finally, we have eq. (7), which here becomes

$$G_3(t) = \frac{3KE_e + 3KE_g \exp - t/\tau}{9K - E_e - E_g \exp - t/\tau}. \tag{66}$$

These three approximations are compared with $G(t)$ in Figure 24, choosing $G_e = 10$ bar, $G_g = 1000\ G_e$, $K_g = 3G_g$, $K_e = K_g/2$, and $K = K_e$. As expected, $G_1(t)$ underestimates $G(t)$ in the glassy region and in the upper portion of the transition region. It then overestimates $G(t)$ in the center and lower transition. This is brought out more strikingly by the ratio $G_1(t)/G(t)$, also plotted in Figure 24. This overestimation results in a shift of the transition in the shear modulus estimated from the tensile modulus by eq. (64) to longer

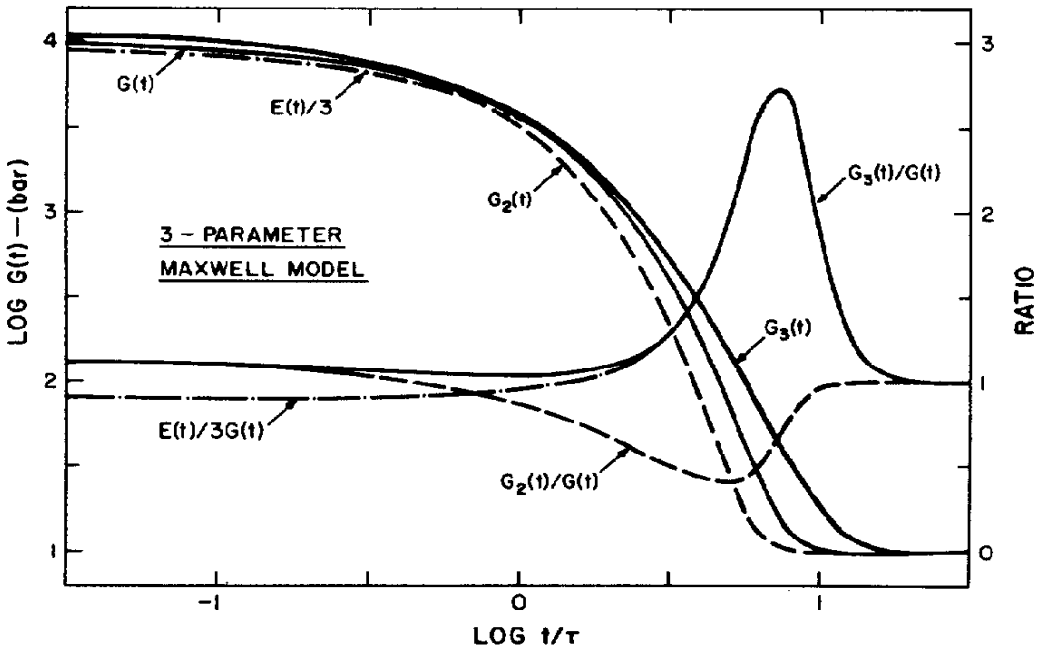

Fig. 24. Log $G(t)$ as function of t/τ; various approximations.

times compared with the true transition. Clearly, $E(t)/3$ is a poor approximation in the transition region.

The behavior of $G_2(t)$, resulting from setting $K(t) = K_e$, is just the opposite. After an initial overestimation of $G(t)$ in the glassy region, $G(t)$ is underestimated (and the transition shifted to shorter times) by $G_2(t)$. As shown by the plot of the ratio $G_2(t)/G(t)$, the underestimation by $G_2(t)$ is less than the overestimation by $G_1(t)$ in the transition region.

$G_2(t)$ can be obtained only if an analytic, Laplace-transformable expression is available for $E(t)$. The advantage of $G_2(t)$ over $G_1(t)$ is lost when the inexact inversion leading to eq. (7) is used. Compared to $G_1(t)$, $G_3(t)$ overestimates $G(t)$ in the glassy and upper transition region but then merges with $G_1(t)$. All four curves merge, of course, in the rubbery (equilibrium) region.

It should be noted that setting $K(t) = K_g$ instead of K_e (the results are not shown) gives the correct estimate in the glassy region, but the behavior in the transition region is closely the same in both cases. In any case, values of K_g are not generally available at present.

It may be conjectured that these simple model calculations present qualitatively the same behavior as that which may be expected from real materials. Thus, we expect eq. (7) to overestimate the value of the shear modulus and to shift the transition to longer times than those at which it would appear in direct measurements. While eq. (7) does not appear to be an improvement on $E(t)/3$ in the isothermal–isobaric estimation of $G(t)$ from $E(t)$ data, it does allow the temperature and pressure dependence of the bulk modulus to be taken into account.

The authors gratefully acknowledge support of this work by the National Science Foundation, the supplies of samples by the E. I. DuPont de Nemours Company, and last, but not least, advice and helpful discussions with Professor R. W. Vaughan and Mr. W. V. Chang.

References

1. P. W. Bridgman, *The Physics of High Pressure*, G. Bell and Sons, London, 1949.

2. A. J. Matheson, *J. Chem. Phys.*, **44**, 695 (1966).

3. M. S. Patterson, *J. Appl. Phys.*, **35**, 176 (1961).

4. J. M. O'Reilly, in *Modern Aspects of the Vitreous State*, J. D. Mackenzie, Ed., Butterworths, London, 1964.

5. J. D. Ferry, *Viscoelastic Properties of Polymers*, John Wiley and Sons, New York, 1970.
6. E. J. Parry and D. Tabor, *J. Mater. Sci.*, **8**, 1510 (1973).
7. J. D. Ferry and R. A. Stratton, *Kolloid-Z.*, **171**, 107 (1960).
8. M. L. Williams, R. F. Landel, and J. D. Ferry, *J. Amer. Chem. Soc.*, **77**, 3401(1955).
9. F. Bueche, *J. Chem. Phys.*, **36**, 2940 (1962).
10. J. M. O'Reilly, *J. Polym. Sci.*, **57**, 429 (1962).
11. A. Zosel, *Kolloid-Z.*, **199**, 113 (1964).
12. E. J. Parry and D. Tabor, *Polymer* **14**, 617 (1973); **14**, 623 (1973); **14**, 629 (1973).
13. P. R. Billinghurst and D. Tabor, *Polymer*, **12**, 101 (1971).
14. K. L. DeVries and D. K. Backmann, *Polym. Lett.*, **9**, 717 (1971).
15. H. Sasabe, Ph.D. dissertation, Tokyo University, 1972.
16. J. E. McKinney, H. V. Belcher, and R. S. Marvin, *Trans. Soc. Rheol.*, **4**, 347 (1960).
17. R. S. Marvin and J. E. McKinney, in, *Physical Acoustics*, Vol. 2B, W. P. Mason, Ed., Academic Press, New York, 1965.
18. P. W. Bridgman, *Proc. Amer. Acad. Arts Sci.*, **76**, 1 (1945).
19. C. E. Weir, *J. Res. Nat. Bur. Stds.*, **46**, 207 (1951); **53**, 245 (1954).
20. L. A. Wood, *Polym. Lett.*, **2**, 703 (1964).
21. V. Bianchi, A. Turturro, and G. Basile, *J. Chem. Phys.* **71**, 3555 (1967).
22. K. H. Hellwege, W. Knappe, and P. Lehmann, *Kolloid-Z.*, **183**, 110 (1961).
23. M. Breuer and G. Rehage, *Kolloid-Z., u. Z. f. Hochpolymere*, **216**, 159 (1967).
24. G. Goldbach and G. Rehage, *Rheol. Acta*, **6**, 30 (1967).
25. A. Quach and R. Simha, *J. Appl. Phys.*, **42**, 4592 (1971).
26. R. W. Warfield, Polym. *Eng. Sci.*, **6**, 176 (1966); *Macromol. Chem.*, **116**, 70 (1968).
27. J. E. McKinney and M. Goldstein, *J. Res. Nat. Bur. Stds.*, **78A**, 331 (1974).
28. S. V. Radcliffe, in, *Deformation and Fracture of High Polymers*, H. H. Kausch, J. H. Hassel, and R. I. Jaffee, Eds., Plenum Press, New York, 1973, p. 191.
29. A. C. Stevenson, in, *Vulcanization of Elastomers*, G. Alliger and I. J. Sjothun, Eds., Reinhold Publishing Co., New York, 1964, p. 265.
30. S. E. Babbs and G. J. Scott, *Rev. Sci. Instr.*, **36**, 1456 (1965).
31. D. M. Warschauer and W. Paul, *Rev. Sci. Instr.*, **29**, 675 (1958).
32. R. W. Fillers, Ph.D. dissertation, California Institute of Technology, Pasadena, California, 1975.
33. N. G. McCrum, B. E. Read, and G. Williams, *Anelastic and Dielectric Effects in Polymeric Solids*, Wiley, New York, 1967.
34. S. C. Sharda and N. W. Tschoegl, *Trans. Soc. Rheol.* (in press).
35. P. J. Blatz, in, *Rheology, Vol. V.*, F. Eirich, Ed., Academic Press, New York, 1969; Rubber Chem. Techn. **36**, 1459 (1963).
36. P. J. Blatz, in, *Polymer Networks: Structural and Mechanical Properties*, A. J. Chompff, Ed., Plenum Press, New York, 1971.
37. J. R. Richards, R. G. Mancke, and J. D. Ferry, *Polym. Lett.*, **2**, 197 (1964).

38. M. Goldstein, *J. Chem. Phys.*, **39,** 3369 (1963).
39. A. B. Bestul, *Glastech. Ber., Sonderband 32K*, **VI,** 59 (1959).
40. A. B. Bestul and S. S. Chang, *J. Chem. Phys.*, **40,** 3731 (1964).
41. A. K. Doolittle, *J. Appl. Phys.*, **22,** 1471 (1951); **28,** 901 (1957).
42. F. D. Murnaghan, *Finite Deformation of an Elastic Solid*, Wiley, New York, 1951, p. 68.
43. P. Tait, *Physics and Chemistry of the Voyage of H. M. Ship Challenger*, Vol. II., Cambridge University Press, Cambridge, 1900, p. 1.
44. L. A. Wood, *J. Polym. Sci.*, **B2,** 703 (1969).
45. A. Peterlin, *J. Macromol. Sci.-Phys.*, **B11(1),** 57 (1975).
46. S. F. Kurath, E. Passaglia, and R. Pariser, *J. Appl. Polym. Sci.*, **1,** 150 (1959).
47. K. Frensdorff, E. I. duPont and de Nemours Co., Wilmington, Delware, private communication.
48. T. P. Yin and R. Pariser, *J. Appl. Polym. Sci.*, **8,** 2427 (1964).
49. P. Heydemann and H. D. Guicking, *Kolloid-Z.*, **193,** 16 (1963).

Received January 26, 1976
Accepted as revised May 26, 1976